Nuclear Transparency in Double Scattering Processes

December 19, 1995

W.K. Brooks, V.D. Burkert, B.A. Mecking, M.D. Mestayer
B. Niczyporuk, E.S. Smith, and A. Yegneswaran
CEBAF, Newport News, VA, USA

M.I. Strikman
Pennsylvania State University, University Park, PA, USA

L.L. Frankfurt
Tel Aviv University, Ramat Aviv, Tel Aviv, Israel

W.R. Greenberg
CDC Investment Management Corp. 9 W. 57th Street, New York, NY 10019 USA

G.A. Miller
University of Washington, Seattle, USA

B. Quinn
Carnegie-Mellon University, Pittsburgh, PA, USA

D.S. Armstrong, H.K. Egiyan, K.A. Griffioen
The College of William and Mary, Williamsburg, VA, 23187, USA

M.J. Amaryan, G.A. Asryan, R.A. Demirchyan, K.Sh. Egiyan,
M.S.Ohanjanyan, M.M. Sargsyan, Yu.G. Sharabian, S.G. Stepanyan
Yerevan Physics Institute, Yerevan 375036 Armenia

S.E. Kuhn
Old Dominion University, Norfolk, VA 23529

CEBAF Large Acceptance Spectrometer Collaboration

Spokespersons: K.Sh. Egiyan, K.A. Griffioen, M.I. Strikman

Update Synopsis

This proposal is an updated version of PR-94-019 which was presented to PAC8 on June 13-17, 1994. The advisory committee deferred this proposal because of possible problems in understanding the theory of the double scattering mechanism in $A(e,e'pN)X$ reactions. The potential problems addressed by PAC8 were:

- competing meson exchange current mechanisms;
- correlation effects;
- sensitivity to model parameters, two body potentials, and relativistic effects;
- sensitivity to the two-body correlations resulting from realistic two-body potentials.

The updated proposal addresses these points.

The incident electron beam energy has been changed from 4 GeV to 6 GeV, now that proposals at 6 GeV are acceptable. The higher beam energy extends the range of momentum transfer to $Q^2 \approx 6$ GeV^2, where color transparency effects are much larger.

The focus has shifted toward deuterium and ^{3}He targets, with supplementary measurements using ^{4}He targets. This reflects the significant recent theoretical progress in understanding the pattern of color coherence effects in exclusive high-Q^2 reactions on the deuteron.

Abstract

We propose to measure the ratio of the cross sections of the $(e,e'NN)$ and $(e,e'N)$ reactions, as well as the ratio of the $(e,e'NN)$ cross section observed at the kinematics dominated by double scattering to the cross section of the same process measured at the kinematics dominated by screening. In both reactions, a high momentum nucleon will be detected in the direction of the virtual photon (forward kinematics). In the $(e,e'NN)$ reaction the second nucleon (N) will be detected in rescattering kinematics. In the case of the deuteron, determination of $d(e,e'pn)$ would be performed both via the study of recoil protons and via the detection of the forward proton. The same triggers would allow us to study reactions such as $d(e,e'pN^*(\Delta))$ with $N^*(\Delta)$ either produced with momentum $\sim \vec{q}$ or nearly at rest. The light nuclei d, ^{3}He and ^{4}He will be used as targets at the CEBAF Large Acceptance Spectrometer (CLAS). The measurement of double scattering events determines the probability for the nucleon struck by the electron **to interact** at small internucleon distances of about 1 fm. This approach is complementary to more traditional studies of color transparency which have been focused on measuring the probability that the struck nucleon **does not interact**.

The proposed measurement will test the paradigm of color transparency physics, that a small-sized wave packet expands as it moves through the nucleus. Indeed, current theoretical studies using realistic models of the nucleon show that a wave packet produced in a hard reaction is small—the long ranged soft pion and gluon fields are suppressed. A small sized wave packet is likely to be formed for values of Q^2 as low as $2-3$ (GeV/c)^2. This wave packet quickly evolves inside the nucleus, so that the sensitivity to the initial small size is often lost. However, rescattering processes on light nuclei occur after the wave packet has traveled a single internucleon distance. Thus, the rescattering depends on whether the produced wave packet was small. Our estimates show that the onset of suppression of final state interactions due to Chiral and Color transparency effects occurs at energies available at CEBAF.

The plan is to make a systematic analysis of the $(e,e'NN)$ and $(e,e'N)$ reactions over the full range of Q^2 starting from $Q^2 \approx 1$(GeV/c)^2. The lower Q^2 range will allow us to check the theoretical understanding of standard multiple scattering effects, including corrections caused by two-nucleon correlations and meson exchange currents. This would help to constrain the analyses at higher values of $Q^2 = 4-6$ (GeV/c)^2. The elaborate tests of the eikonal approximation for electron nucleus scattering which would be performed in the course of the proposed analysis for $Q^2 < 3(GeV/c)^2$ will help to improve the reliability of interpretation of the $(e,e'p)$ color transparency experiments planned at CEBAF.

The price to pay for switching from nearly exclusive kinematics in the $A(e,e'p)(A-1)^*$ process to the detection of two hadrons in the final state is a substantially smaller cross section. The use of large acceptance detectors like CLAS is necessary.

1. Introduction

The absorption of a high momentum photon leads to the production of a small sized wavepacket in which the long range pion and gluon fields are absent. It is interesting to investigate how such a wavepacket moves within the nucleus and how the long-range fields are restored. Such an investigation provides a promising new method for investigating QCD dynamics, for observing quark-gluon degrees of freedom and internucleon forces in nuclei. Similar questions arise in the search for the phase transitions in AA collisions and in constructing the theory of quark-gluon matter evolution in the early universe[1].

1.1. Color Coherent Effects in Perturbative QCD

The physics of the wave packet and its expansion with time is vital for determining whether or not color transparency may occur in nuclear quasielastic reactions. Recall that Mueller and Brodsky[2,3] used perturbative QCD to suggest that small sized configurations provide the dominant contributions to the nucleon form factor and, therefore the final state interaction will disappear with increasing Q^2. This interesting prediction has been proven in perturbative QCD[4] by calculating the effects of Sudakov type form factors which suppress the contribution of large size configurations.

The consideration of pQCD diagrams led to the suggestion[2,3] that the A-dependence of quasi-exclusive processes

$$l(h) + A \to l(h)' + p + (A-1) \tag{1}$$

could be used to determine the configurations that dominate in hard two-body reactions. The notion was to explore the color screening phenomenon in QCD—the decrease of the interaction with a decrease of the transverse area, $S = \pi b^2$, occupied by the color charge: $\sigma \sim S$ for $b^2 \ll < r_t^2 >$. Here $< r_t^2 >$ is the mean square of the transverse size of the nucleon. This color screening phenomenon has been observed indirectly in the existence of Bjorken scaling[5] and in the small cross section of ψN scattering as determined from J/Ψ-meson photoproduction off nucleons and nuclei (see e.g. Refs.[5,6]). More recently this phenomenon was observed in the exclusive vector meson production at HERA[7,8,9].

Color screening would allow a small-sized object to escape from the nucleus without further interactions. Hence, up to small effects due to the suppression of point like configurations (PLCs) in a nucleon bound within a nucleus[7,8], the cross section of reaction (1) would be proportional to A. The prediction of a spectacular change of the A-dependence of the cross section of reaction (1) has led to a number of further theoretical analyses[9–16] and to first attempts to observe the phenomenon using the BNL proton beam[21] and SLAC electron beam[22] and to the ongoing experimental investigations at BNL[23]. Evidence for the onset of color transparency was also reported from vector meson production off nuclei at FNAL[24].

It is worth emphasizing that so far most of the evidence for CT comes from the interaction of $q\bar{q}$ systems which have a direct analog in QED. Observation of CT for the interaction of small qqq system would reflect the nonabelian nature of CT phenomenon in QCD (see

e.g. Ref.[25]). However, the applicability of perturbative QCD to CEBAF energies has been questioned in Refs. [26,27,28] which emphasized the important role of end point (e.g. Feynman type) contributions.

1.2. Color Coherent Effects in Nonperturbative QCD Models of a Nucleon

The suppression of soft modes and the formation of small-size or point-like configurations (PLC) by hard interactions seem to be an essential feature of nonperturbative QCD. Both realistic quark models of the nucleon (which contain a color Coulomb interaction), and Skyrmion models, predict[15] that PLCs are formed at momentum transfers as small as 1-2 $(\mathrm{GeV/c})^2$ and that the long-range pion field is suppressed within a PLC[29] (see e.g. Fig. 1). As a consequence the PLC may be a **precursor** of pQCD. The opposite behavior is expected in mean-field quark-models of the nucleon where the interaction between quarks is described by an oscillator potential[15]. Thus, one pressing problem is to find experimental evidence that helps to distinguish between these two classes of models.

1.3. Wave packet expansion

Although small-sized wave packets may be produced at low values of Q^2, interactions are suppressed only when the coherence length of geometrical color optics exceeds the nuclear radius R_A[29]:

$$l_{coh} = \frac{2\nu}{(M^{*2} - m_N^2)} \gg 2R_A. \tag{2}$$

Here M^* is the mass of the intermediate state important in the calculation of the nucleon form factor, and ν is the energy transferred to the nuclear system. When the condition of Eq. 2 is violated, the produced hadron expands rapidly within the nucleus, and the final state interaction is restored. For heavy nuclei Eq. 2 requires unrealistically large Q^2, since the nuclear radius is large on the scale characteristic of color phenomena. Furthermore, in perturbative QCD, M^{*2} increases with Q^2. One cannot escape this problem by using light nuclei. This is because not much absorption is expected, so the effect of CT in the Eq. 1 must be small, and on the order of the various uncertainties in the calculation. Thus, the effects of wave packet expansion seem to obscure to a large extent the pQCD CT physics of Eq. 1.

Let us make some simple numerical estimates[13] of l_{coh}. A realistic estimate of $M^{*2} - m_N^2$ for color fluctuations is between m_ρ^2 and $1/\alpha'$ (α'=0.9 GeV^{-2} is the slope of the nucleon Regge trajectory). Thus Eq. 2 can be rewritten as:

$$L_{coh}(\mathrm{fm}) \sim l_0(\mathrm{fm}) \cdot p_N(\mathrm{GeV/c}), \qquad l_0 = 0.35 - 0.55 \text{ fm} \tag{3}$$

where p_n is the wave packet momentum. In the following estimates, we will adopt an optimistic value of $l_0 = 0.5$ fm. Choosing l_0 in the lower end of the range would correspond to rescaling Q^2 by approximately a factor of 1.5, say from $Q^2 = 4 - 6$ $(\mathrm{GeV/c})^2$. In reaction (1) $p_N = \sqrt{Q^2 + (Q^2/2m_N)^2}$, so the color coherence effect of the change of A_{eff}/A

in this process is washed out by the quantum mechanical diffusion of the wave packet[13,29] up to $Q^2 \approx 10$ (GeV/c)^2. Therefore, in reactions like $A(e,e'p)$ very large values of Q^2 are necessary to establish CT. This expectation is consistent with the recent SLAC experiment NE18[22] which does not show a considerable change in A_{eff}/A at their current level of accuracy ($\approx 10\%$) up to $Q^2 \approx 7$ (GeV/c)^2. At the same time, a small variation of the nuclear transparency for the kinematics of NE-18, expected for the value of l_0 adopted in our estimates, is consistent with the data (see Section 2). Larger changes of the nuclear transparency observed in the BNL (p,2p) experiment[21], are also consistent (because of the higher momenta of protons involved in the $(p,2p)$ reaction (larger l_{coh}) and the presence of one proton in the initial and two protons in the final state) with such a small variation in $(e,e'p)$, see the discussion in Ref. [29].

To summarize, for Q^2 accessible at CEBAF, l_{coh} does not exceed 1–2 fm. Thus, the practical problem which emerges in searching for the effects of small-sized wave packets is that the PLC expands rapidly (even if selected by a hard probe at the interaction point) to the size of a normal hadron while propagating through nuclei. We shall argue that measuring double scattering processes in light nuclei provides a solution to this problem.

1.4. Nuclear Effects

There are several distinctive features of nuclei as dynamical systems of nucleons which might affect nuclear transparency and obscure CT effects.

The first are the correlations between nucleons. It was observed in the 1960's-1970's by Moniz, Nixon, and Walecka[30], and by Yennie[31] that correlations might significantly change the nuclear transparency. These papers used the Glauber approximation to demonstrate that correlations in coherent hadron-nucleus scattering make a nucleus less transparent, whereas in the case of noncoherent reactions the correlations increase the transparency of nuclei for rescattering at large angles by as much as $\approx 30\%$[31].

Recently, this problem has been reviewed by the several authors[18,19,32,33] within the context of the investigation of color transparency. Refs.[18,19] suggested a modification of the optical model approximation to include correlations. They found that correlations may significantly (20%) increase the cross section of the reaction in Eq. 1 and considerably suppress the onset of CT effects especially at intermediate Q^2. However, in the other studies[32,33,34] the effects of correlations were estimated to be no more than 5%.

One way to suppress the correlation effects and speed up the onset of CT, is to restrict the excitation energies of the final state in the $(e,e'p)$ reactions to ≤ 50 MeV (see Ref.[34]).

To get a better understanding of the correlation effects, it is natural to perform detailed investigations with the lightest nuclei d, ^{3}He and ^{4}He, for which most realistic calculations of nuclear wave functions are available[36,37,38,39,40] and restrict the analysis to the kinematics where predictions of different wave functions for the same nucleus differ negligibly as compared to the size of the predicted CT phenomena.

In addition, it is natural to investigate correlation effects in nuclear transparency starting at $Q^2 = 1-2$ (GeV/c)^2 where the CT effects are expected to be negligible and where the

Glauber approximation provides a reliable framework[41] for calculating the effects of FSIs.

There are other effects which one must consider. One is a possible nuclear medium modification of nucleon properties, an off-shell effect. These effects are likely to depend on Q^2 and may mask[20,42] the color transparency effects for intermediate Q^2. Possible solutions include trying to disentangle these effects via a detailed study of the momentum dependence of the transparency of the $A(e,e'p)$ reaction and measuring the transparency ratios which are less sensitive to the off-shell effects[43], such as the (e,e'pp)/(e,e'p) ratio proposed here.

Meson exchange effects and the Δ-isobar contribution (IC) must also be considered. However, estimations of the contribution from meson exchange currents (MEC) for $Q^2 > 1$ $(\mathrm{GeV/c})^2$ are rather controversial (see e.g. Ref.[44]). The strategy in this case is again to start the measurements with Q^2 as low as ≈ 1 $(\mathrm{GeV/c})^2$, where the ejectile energies are sufficiently large for the eikonal approximation to be reliable (see e.g. Refs.[41,48]) but not too large to apply the conventional partial-wave decomposition including MEC and IC effects[45]. The comparison of the predictions of these two prescriptions for these values of Q^2 allows one to search for the kinematics where double scattering is enhanced and MEC and IC are suppressed as well as for the kinematics where MEC and IC effects are enhanced. The experimental study of the later kinematics would ensure that in the kinematics of double scattering these effects are under control. Once the kinematics are identified, the situation at higher Q^2 would be even more advantageous[41] since the MEC contribution is suppressed at $x = Q^2/2m\nu \approx 1$. The IC contribution would be suppressed[46] as well because of the probable rapid decrease of the $\gamma^* N \to \Delta$ transition form factor with Q^2 and also the fact that $NN \to N\Delta$ amplitude is predominately real (see Section 2 and Ref.[41] for details). Note that the situation is even more advantageous for two proton emission from ^{3}He and ^{4}He targets. In this case the contribution of MECs from a pp pair is negligible[47].

2. Physics Motivation

The main conclusions of the previous sections are:

1. Coherent effects may only reveal themselves for $Q^2 \leq 6$ $(\mathrm{GeV/c})^2$ at distances ≤ 2 fm. Thus, it would be difficult to establish these effects reliably using $(e,e'N)$ reactions only. We need to add new, complementary processes which probe the hadron within 2 fm of the formation of its small configuration to the list of the studies of nuclear coherent phenomena.

2. The practical strategy to account for the correlation effects in the search for CT is to measure the effects of nucleon correlations on the nuclear transparency at moderate Q^2 and to use these results for the analysis of the high Q^2 data.

3. It is necessary to identify kinematics where that different nuclear effects such as off-shell effects, Δ-isobar contribution, and meson exchange effects are reliably controlled.

2.1. The Idea

The main idea of the proposal is to measure the probability for the ejectile to interact. This should vanish if PLCs are produced by the absorption of the virtual photon. In that

case, the PLC need only propagate one internucleon distance. Such a measurement is complementary to the measurement of the probability "not to interact" as measured in the (e,e'N) processes, but is more sensitive to color-coherent effects.

The measurement of the probability to interact again will be achieved by selecting double scattering kinematics in the reaction

$$e + A \to e' + N_f + (N_r, h_r) + (A-2) \tag{4}$$

where the recoiling nucleon (hadron)- $N_r(h_r)$ with momentum $p_r \geq 300 - 400$ MeV/c is detected in coincidence with the fast nucleon-N_f ($p_f \approx q \approx$ several GeV/c) and the scattered electron.

To visualize the above statement, in Fig. 2 we present the graphs for the simplest case—scattering off the deuteron. Fig. 2a describes the plane wave impulse approximation (PWIA) term where the struck nucleon does not interact with the spectator nucleon and Fig. 2b corresponds to the situation where a fast moving struck nucleon rescatters elastically off a slow nucleon spectator.

To measure the probability for a fast struck nucleon to interact again we have to choose the kinematics where the overall cross section is dominated by the square of the rescattering amplitude (Fig. 2b), which we will further call the double scattering term. The overall cross section in this case exceeds the value given by the PWIA term. The obvious advantage of Eq. 4 in double scattering kinematics is that it allows us to single out the events where the secondary $N_r(h_r)$ is produced in the interaction of the ejected system with the residual nucleus.

One can also select kinematics (usually corresponding to $p_r \leq 200 - 250$ MeV/c[41]), where the dominant correction to the PWIA cross section comes from screening contribution arising from the interference of PWIA (Fig. 2a) and rescattering (Fig. 2b) amplitudes. This screening term will result in a substantial decrease of the cross section from the value given by the PWIA term only.

The distinctive features of color coherence in double scattering processes include:

- Using light nuclei as targets allows one to satisfy the condition for the color coherence $l_{coh} \geq R_A$ for the lowest possible Q^2. Thus, one can focus on probing the PLC interaction at the distance scales of 1 fm where expansion effects are minimal.

- Color coherent effects are observable as a decrease, with increasing Q^2, of the final-state interaction probability from the value predicted by the Glauber theory. As a result the relative change of the cross section is much larger than in the A(e,e'p) case, where the nuclear transparency is close to unity.

- The double scattering cross section for $A(e, e'NN)$ process is more sensitive than the $(e, e'N)$ cross section to the transverse spatial size, b, of the PLC wave packet. This is because the cross section depends on the interaction between the PLC and a nucleon, and rescattering is proportional to the square of the amplitude which should decrease with Q^2. In the $(e, e'p)$ reactions CT effects are proportional to the first power of this amplitude.

Simultaneous measurement of the $(e, e'NN)$ cross section in the kinematic region dominated by screening effects and for kinematics dominated by the double scattering effect allows us to address several other important features.

- The ratio of the cross sections measured at the kinematics where double scattering dominates to the cross section measured at the kinematics where screening effects dominate, will have extra sensitivity to color coherent effects, since they would decrease the numerator and increase the denominator of this ratio.
- Measurement of this ratio has several experimental advantages—smaller normalization uncertainties, simpler radiative corrections, etc.

2.2. Methods of Calculations

A model of the time evolution of the PLC is required to estimate the magnitude of the expected nuclear coherence effects. One may use the quark-gluon basis or a hadronic basis[29]. We will use both methods in our analysis.

The use of the quark-gluon basis leads to the quantum diffusion model (QDM) of Ref.[13]. Here one approximates the evolution of the wave packet by averaging over its transverse size at a given distance l from the production point. As a result, one can estimate the effective total cross section $\sigma_{tot}(l, Q^2)$, for the interaction of PLC with target nucleons, at the distance l as

$$\sigma_{tot}(l, Q^2) = \sigma_{tot}\left\{\left(\frac{l}{l_h} + \frac{\langle r_t(Q^2)^2\rangle}{\langle r_t^2\rangle}(1 - \frac{l}{l_h})\right)\Theta(l_h - l) + \Theta(l - l_h)\right\} \tag{5}$$

where $l_h = 2p_f/\Delta\ M^2$, and $\Delta\ M^2 = 0.7 - 1.1$ GeV^2. Here $\langle r_t(Q^2)^2\rangle$ is the average squared transverse size of the configuration produced at the interaction point. In several realistic models[15] it can be approximated as $\langle r_t(Q^2)^2\rangle/\langle r_t^2\rangle \sim 1$ GeV$^2/Q^2$ for $Q^2 \geq 1.5$ GeV^2. Since we are interested in the effect of elastic rescattering we also need to model the elastic amplitude. Generalizing the optical theorem by allowing the total cross section to depend on l leads to the following relation for the NN elastic scattering amplitude:

$$f^{NN}(k_t, Q^2, l) \approx \sigma_{tot}(l, Q^2) \cdot e^{\frac{B}{2}t} \cdot \frac{G_N(t \cdot \sigma_{tot}(l, Q^2)/\sigma_{tot})}{G_N(t)} \tag{6}$$

where B is the slope of elastic NN-amplitude and, $G_N(t)$ ($\approx (1 - t/0.71)^2$) is the Sachs form factor. The last factor in Eq. 6 accounts for the difference between elastic scattering for point-like and average configurations, which is based on the observation that the t dependence of $d\sigma^{h+N\to h+N}/dt \sim\ G_h^2(t) \cdot G_N^2(t)$. It is obvious from this equation that elastic rescatterings are much more sensitive to the change of the effective interaction cross section.

The time development of the PLC can also be obtained by modeling the ejectile-nucleus interaction as $\hat{U} = -i\sigma(b^2)\rho(R)$, Then one can assume a baryonic basis and compute the

relevant matrix elements of $\sigma(b^2)$ [14] using the wave functions. Another approach is to use a finite basis to model the matrix elements of $\sigma(b^2)$. We adopted a three-component model which describes PLC as a coherent superposition of 3 states N, N^* and N^{**} (the latter representing the continuum)[35]. This explicitly imposes the condition that the wave packet produced initially interacts weakly and also uses information from diffractive NN scattering to constrain the model parameters. Both treatments of PLC expansion use parameters which yield predictions consistent with the nearly flat transparency observed in the NE18 experiment (see Fig. 3) and with the positive signal observed in the BNL experiment[21].

We start with considering the double scattering process in the $d(e, e'pn)$ reaction for which we have performed detailed theoretical calculations[41,48] using realistic wave functions and considering a large range of theoretical effects which can affect the onset of color transparency.

For the first analysis of double scattering processes on ^{3}He and ^{4}He targets we used simplified harmonic oscillator wave functions[43], with the high momentum component described using a two nucleon correlation model[49]. Recently we developed a complete eikonal description of the break up of the lightest nuclei. Numerical calculations using realistic ^{3}He wave functions accounting for the short-range nuclear correlations and including higher order rescatterings are under way[50].

The calculations we performed[41,43] clearly demonstrate the merits of the $(e, e'NN)$ reaction discussed above for the investigation of color coherent effects at intermediate Q^2. The results of these calculations will be used in the next section to estimate the minimal Q^2 necessary to observe evidence for nuclear coherence effects.

It is of utmost importance in the absence of CT effects for $Q^2 < 3$ GeV^2 (confirmed in all above calculations) that we check thoroughly the eikonal picture of rescatterings and nucleon correlations in the double scattering processes. One should emphasize that for nucleon energies above 1 GeV corresponding to $Q^2 \geq 2$ (GeV/c)^2, the elementary nucleon amplitude weakly depends on energy. Hence for these values of Q^2, the eikonal model predicts practically energy-independent shapes of the spectra. Measurements at lower energies are essential for interpreting the data at larger Q^2.

2.3. Measurement Method

To measure nuclear transparency we need quantities which more directly indicate the extent to which the nucleus is transparent.

Previously, the quantity that has been used in $(p, 2p)$ (Ref.[21]) and $(e, e'p)$ (Ref.[22]) reactions to estimate transparency was the ratio of the experimentally measured cross section to the corresponding cross section calculated within the plane wave impulse approximation (PWIA) (for theoretical motivation see e.g. Refs.[13,16]):

$$T = \frac{\sigma(e, e'p)^{exp}}{\sigma(e, e'p)^{pwia}} \tag{7}$$

where $T \to 1$ corresponds to complete nuclear transparency.

We propose to measure the following quantities which will allow us to determine how strongly nucleons propagating in a nucleus experience FSIs:

- The ratio of the experimentally measured cross section of $(e, e, N_f N_r)$ processes to the same cross section calculated within PWIA (see e.g. Fig.2a):

$$T^{double}(Q^2, p_f, p_r) = \frac{\sigma^{exp}_{(e,e'NN)}}{\sigma^{PWIA}_{(e,e'NN)}}, \tag{8}$$

  where $\vec{p}_f$ and $\vec{p}_r$ are the fast knocked-out and slow recoil nucleons.

- The ratio of the experimental cross section for $(e, e' N_f N_r)$ measured for the kinematics dominated by double scattering to the cross section measured for the kinematics dominated by screening effects.

$$R(Q^2, p_{r1}, p_{r2}) = \frac{\sigma^{double}(p_{r1})}{\sigma^{screen}(p_{r2})}, \tag{9}$$

where $p_{r1} > 300\ MeV/c$ is the recoil nucleon momentum, in the kinematics where double scatterings dominates and $p_{r2} < 300\ MeV/c$ is the same nucleon momentum in the kinematics where screening effects are dominant. Both $T^{double}(Q^2, p_f, p_r)$ and $R(Q^2, p_f, p_r)$ approach the values predicted in PWIA, provided that complete nuclear transparency occurs. However, the ratio defined by Eq. 9 is more sensitive to the effects of color transparency since these effects cause the numerator to decrease and the denominator to increase.

Another experimental advantage is that Eq. 9 represents the ratios of quantities measured within the same experimental run. Obviously, this avoids many problems (such as the necessity to calculate a denominator of T in Eq. 7, radiative corrections, etc.).

Instead of Eq. 9 one can also analyze the similar ratio with denominator substituted by the cross section of the $(e, e'p)$ reaction for $x = 1$ and $p_f < 200\ MeV/c$ (which also would be measured in the experiment) which is described by the PWIA term with screening corrections.

Fig. 4 illustrates these points. T^{double} is calculated for $d(e, e'pn)$ within the eikonal approximation without color transparency. The figure shows that for $x \approx \alpha = (E_r - p_r^z)/m \approx 1$ and transverse momenta $p_t \leq 250\ MeV/c$, FSIs are dominated by screening effects ($T^{double} < 1$), whereas for $p_t \geq 350 - 400\ MeV/c$ double scattering dominates ($T^{double} > 1$).

Fig. 5 shows the relative effect of CT calculated within the QDM and three resonance models, normalized to the Glauber approximation. Fig. 6 reveals a substantially larger sensitivity to CT effects in the quantity R of Eq. 9.

As mentioned above in our calculations of the $(e, e'NN)$ process on ^{3}He and ^{4}He, we used a simplified model for nuclear wave functions and more elaborate calculations are in progress. However, within these models of wave functions we observe noticeable sensitivity to CT effects similar to the one we found in the deuteron case.

This point is demonstrated in Fig. 7 where calculations of CT for T, T_{double}, R (for the case of quasielastic $(e, e'p)$ and $(e, e'p_f, p_r)$ reactions on ^{4}He are normalized to the

corresponding quantities computed within the Glauber approximation. The calculation was performed for the kinematics where $\vec{p}_f \sim \vec{q}$ ($\vec{q}$ - momentum of virtual photon) and $|\vec{q}| \gg |\vec{p}_r| \approx 0.4$ GeV/c (for details of the kinematics see next section). The effect of deviations from the Glauber calculation is the smallest for T (solid curves), larger for T_{double} (dashed curves), and largest for the R ratios (dotted curves). These figures demonstrate that color transparency strongly influences the double scattering process, even at intermediate Q^2.

We find very similar results for the same reactions on ^{3}He in the three-state model, so we display only results for the R ratios in Fig. 8. This model also illustrates that interesting information can be obtained from studying double scattering events with a leading nucleon resonance. Study of reactions producing leading resonances will be performed using two methods—one is the detection of the recoil proton in the reaction $e + d \rightarrow e + N^* + p_r$, another is the direct observation of the decay products of nucleon resonances. CLAS design has excellent acceptance for many of these channels. Studies of these processes at intermediate $Q^2 \leq 2$ (GeV/c)^2 are also of great interest to determine the properties of the N^*-nucleon interaction. Since the resonances have very different coordinate wave functions their interactions with nucleons could be strongly state-dependent.

Of special interest would be the study of the leading Δ^{++} or Δ^-, for example in e+^{4}He $\rightarrow e + \Delta^{++} + nnn$. This process is forbidden in PWIA approximation, but can occur due to pion exchange of a knockout proton (Δ^+) with the second nucleon. This may be a good way to study chiral transparency—suppression of the pion field of the ejectile[29]. Another promising direction we plan to pursue is the study of reactions where a slow resonance is produced together with a leading proton:

$$e + d \rightarrow e + p_f + N_r^*(\Delta_r^0) \tag{10}$$

This process cannot occur in the impulse approximation, and has specific kinematics characteristic for double scattering as it strongly peaks at $\alpha(N^*) \approx 1$. It can be studied via detection of the forward nucleon with supplementary measurements of the decay products of $N^*(\Delta)$ to determine the quantum numbers of the recoil system. The color transparency effect for this process for all transverse momenta of recoil inelastic state - p_{rt} is as large as for double scattering. Moreover, the rescattering diagrams in the case of inelastic recoil are sensitive to the smallest longitudinal distances compared to elastic recoil[48]. As a result one expects suppressed effects of PLC expansion. In Fig. 9 the comparison of $d(e,e'N)N$ and $d(e,e'N)\Delta$ cross sections using eikonal and CT approximation shows how much one gains sensitivity to CT effects by considering the slow inelastic recoil production. Studies along these lines would be natural once an understanding of the simpler process discussed here is achieved.

Since the double scattering events tag the two-body components of the ground state wave function[34] it is natural to expect that the quantities defined above are sensitive to the short and medium range correlations between the two detected nucleons. Properly defined kinematics allow us to suppress the effects of short range correlations. Nevertheless, under average conditions, bound nucleons in nuclei are surrounded by a hole due to medium-range

($\leq$ 2 fm) nucleon correlations and the two-body densities in the nucleus are not uniformly distributed as a function of the relative distance of any two nucleons[18,51]. This is the reason why the measurement of these reactions must necessarily start at $Q^2 \approx 1$ where no CT effects are expected, and the eikonal approximation of multiple scattering already provides a reliable basis of calculation.

2.4. Theoretical uncertainties

We considering now several theoretical issues which might influence the reliability of our interpretation of the measured cross sections. We are discussing primarily the process of scattering off a deuteron target, since a detailed analysis[41] exists. However, most of the points considered below are relevant for ^{3}He and ^{4}He as well.

2.4.1. Relativistic motion of target nucleons

The fact that high energy processes develop along the light-cone can be taken into account within the framework of light-cone mechanics[11,12]. The light-cone calculation of processes involving a deuteron target is more straightforward than using nonrelativistic quantum mechanics, since the kinematics for the process is written simpler in light-cone coordinates. However, when $x \approx \alpha \approx 1$ (perpendicular kinematics), the uncertainties[41] resulting from neglecting relativistic effects of nucleon motion in the deuteron are insignificant corrections ($\sim \mathcal{O}(1-\alpha)^2$). The relativistic effects are even less important for the FSIs, since the integrals over nucleon momenta in the FSI amplitude are sensitive to smaller values of the deuteron internal momenta when $x = 1$ and $p_{rt} \leq 400$ MeV/c.

2.4.2. Uncertainties in the knowledge of the deuteron wave function

Possible uncertainties in the calculation of the $d(e,e'p)n$ processes with polarized and unpolarized targets are small and under control for the kinematics considered here because nucleon momenta in the deuteron do not exceed $300-400$ MeV/c and FSI terms are sensitive to smaller deuteron internal momenta. Another reason why our processes are less sensitive to the uncertainty of the deuteron wave function, is that we consider observables which are the ratios of experimental quantities in (nearly) similar kinematical conditions (see Eq. 9) for different energies. Besides, the same reaction for parallel ($\alpha \approx 2$) and antiparallel ($\alpha \approx 0$) kinematics has a larger sensitivity to the deuteron wave function and could be used to reduce this uncertainty even further. We anticipate that dedicated experiments to measure wave functions of the lightest nuclei, which are planned at CEBAF as well as currently running at other electron machines, will determine the wave functions with an uncertainty of few percent.

2.4.3. Off-shell effects

The target nucleons are bound in the deuteron; the square of their four momentum is not the square of their mass. One needs to estimate the influence of this effect to calculate the cross sections. We estimated the uncertainties due to these effects by considering the PWIA amplitudes of models[52,12,53] which account differently for off-shell effects in σ_{en}. The differences are very small, less than one percent or so.

Another source of uncertainty arises from the deformation of the bound nucleon wave function. This deformation has been calculated[10] for processes dominated by PLCs. The major effect is the suppression of the probability for PLCs in the bound nucleon due to color screening[12].

In Fig. 10 we present calculations of the ratio defined in Eq. 9 which include the influence of the PLC suppression according to the color screening effect[12], as well as effects (off-shell, relativistic, deuteron wave function) discussed above. The figure demonstrates that uncertainties are on the level of 5%.

2.4.4. Meson exchange currents (MEC) and Δ-isobar contributions

Estimates of contributions from meson exchange currents are rather controversial at large Q^2 since these terms are very sensitive to the assumed t-dependence of the meson-nucleon vertex form factors. These form factors are not obtained from theory; instead they are used as fitting parameters[44]. On the other hand the restriction to $x = Q^2/2mq_0 \approx 1$ and $Q^2 \geq 1$ (GeV/c)^2 strongly suppresses the sea quark content in nucleons. Including mesonic components is one way to treat the anti-quark content, so that a suppression of the sea can be considered as a hint of the suppression of MEC at large Q^2 and $x \geq 1$. This argument relies on the Bloom-Gilman duality[54] between the structure function of a nucleon at $x \to 1$ and contribution of resonances and on the fact that this hypothesis describes reasonably near threshold data for deep inelastic eN scattering. Besides, the diagram corresponding to meson exchange currents contains an extra $1/Q^2$ factor as compared to the PWIA (Fig.2a) and the FSI (Fig.2b) diagrams. The Δ-isobar contribution is expected to be small also in the kinematical range suitable for studying CT effects, since the $\gamma^* N \to \Delta$ transition form factor tends to decrease more rapidly with Q^2 than the N^* transition form factors[46]. Another reason for the suppression of the contribution of Δ's is that the $\Delta N \to NN$ amplitude is predominantly real and decreases rapidly with energy (since it is dominated by pion exchange) whereas the FSI effects we study are determined by the imaginary part of the soft rescattering amplitude.

In Fig. 11 we compare predictions of the eikonal approximations for the $d(e,e'p)n$ reaction with results of calculations[45] performed for $Q^2 = 1$ (GeV/c)^2, $\nu \sim 400 - 500$ MeV and spectator momentum $p_r = 400$ MeV/c. The contribution of meson currents and isobars in the kinematics where NN rescattering dominates is small ($\sim 6\%$ for MEC and $\sim 4\%$ for isobar contribution). Comparison of our approach and that of Ref.[45] hints that the Glauber approximation is already applicable for Q^2 as small as 1 (GeV/c)^2. Note that calculations according to Ref.[45] can be considered as the upper limit for the contribution of meson currents. One can also see from Fig. 11 that the relative contribution of MEC and IC effects

is expected to be a factor ≥ 5 larger for emission angles $\theta_n = 100 - 120^\circ$ than for $\theta \sim 60^o$ where double scattering gives the largest contribution. Since cross sections for these two cases would be measured simultaneously, it would obviously help to reduce uncertainties in the contributions of MEC and IC mechanisms.

One important advantage of studying scattering from both the deuteron and a *pp* pair in ^{3}He is the different role of MECs in the two cases. MECs are strongly suppressed[47] in the *pp* case as compared to the *pn* case, because no charge exchange can occur within the *pp* pair.

2.4.5. Charge exchange contribution and spin dependence of the elementary amplitude

In the above analyses we have neglected contributions of terms in which the large longitudinal momentum is first transferred to the neutron which then converts to a proton via a charge exchange process. Since the charge exchange reaction $np \to pn$ is dominated by pion exchange, its amplitude is predominantly real. Therefore, it contributes primarily to the double interaction term, not to the screening term. Using the data from Ref.[57], we estimate that this correction is of the order of 9% for $Q^2 \sim 2$ GeV^2 and it decreases rapidly with Q^2, approximately as Q^{-4}. For the case of leading neutron production, the relative contribution of the charge exchange is larger by a factor $\sigma^2_{ep}/\sigma^2_{en} \leq 5$. Note that we expect transparency effects to cut down the charge exchange just as they reduce elastic rescattering. This is the chiral transparency effect[15]; so this charge exchange effect does not affect our conclusions concerning the sensitivity of the $d(e,e'p)n$ reaction to color coherent effects.

Note also that we neglected another effect of dependence of the elastic *pn* amplitude on the parallel or anti-parallel nature of the helicities of the colliding nucleons. If we consider, for certainty, magnetic transitions, the rescattered nucleons will predominantly be in the antiparallel (parallel) state for $\lambda_d = 1(0)$. Using the current data on the $\sigma^{tot}_L(pn)$ difference[58], we estimate that this effect leads to a correction to the rescattering amplitude which is $\leq 3\%$ for $Q^2 \sim 2$ (GeV/c)^2 and $\leq 1\%$ for $Q^2 \sim 4$ (GeV/c)^2. It would be straightforward to include these effects in further calculations.

In Fig. 12 we represent the calculation of R^{double} with different values of the parameter ΔM^2 entering into the QDM model of color transparency. Accurate data will, therefore, allow a determination of ΔM^2.

In the scattering off ^{3}He and ^{4}He we select kinematics where only two nucleons are involved (the condition is imposed that the momentum and excitation energy of the $A-2$ spectator system are small). Therefore our analysis of the theoretical uncertainties for the deuteron is equally applicable for the case of these nuclei.

3. Experimental Requirements

For ^2D we will consider the ratio of the $d(e,e'p(n))n(p)$ cross section evaluated in the kinematical range where the dominant mechanism is double scattering to the corresponding cross section where the dominant mechanism is screening. The advantage in the case of the

deuteron target is that it is enough to measure either knock-out or recoil proton to distinguish the necessary kinematical ranges. Thus measurement can benefit from experiments aimed to measure the high Q^2 neutron form factor with slow recoil protons and experiments looking for production of fast knock-out protons in the forward hemisphere.

For ^{3}He and ^{4}He targets the experimental requirements are to measure the ratio of double scattering quasielastic cross section for the $(e, e'p_f p_r)$ reaction (where the (p_f) - forward knocked-out proton and (p_r) - rescattered secondary proton are detected in coincidence with the scattered electron - (e')) to the $(e, e'p_f)$ cross section where $\vec{p}_f \approx \vec{q}$.

The $(e, e'p_f p_r)$ reactions from a ^{3}He target have the advantage that the pp pair wave function has a node in its momentum distribution, so that by choosing the recoil proton momentum close to its value at this node one can strongly suppress the contribution from PWIA and interference terms and therefore enhance the contribution from double scattering. Another advantage (discussed above) is the suppressed contribution from meson exchange currents compared to the case of pn pairs.

We consider these measurements a starting point for the development of the double scattering technique and its further expansion to inelastic rescattering with production of final state nucleon resonances.

We expect to use standard D and ^{3}He targets with the CLAS magnet set for in-bending electrons. We require full functionality of all forward EGN and Cerenkov detectors, the TOF scintillators and all three regions of drift chambers. No other additional detectors or modifications are required.

3.1. Kinematics

The kinematics of the $(e, e'p_f, p_r)$ quasielastic reaction is governed by following general requirements:

- To suppress the contribution of inelastic electroproduction and inelastic secondary pp rescattering one must restrict the excitation energy of the residual $A-2$ nuclei to be less than the pion mass. The kinematical requirement in this case is:

$$\nu - T_f - T_r - \frac{p_{A-2}^2}{2M_{A-2}} \leq m_\pi \tag{11}$$

  where ν is the energy of virtual photon, T_f and T_r are the kinetic energies of knocked-out and secondary proton, respectively, and $\vec{p}_{A-2} = \vec{q} - \vec{p}_f - \vec{p}_r$ is the center-of-mass momentum of the residual nucleus.

- To maximize the contribution from rescattering processes, where initial protons have low Fermi momenta and, therefore, the cross section is maximal and less dependent on the nuclear structure of the target, one chooses the kinematics close to the condition:

$$q + 2m \sim p_f + p_r \tag{12}$$

This determines the optimal condition for the energy transferred by scattered electron as $x \equiv Q2/2m\nu \sim 1$, for the momentum of the recoil nucleon: $\alpha = (E_r - p_r^z)/m \approx x$ and for the momentum of the spectator $A-2$ system $\vec{p}_{A-2} = \vec{q} - \vec{p}_f - \vec{p}_r \approx 0$.

- To minimize the contribution of spectator emission from electroproduction on short-range nucleon correlations (SRC) and maximize the effect of elastic rescattering one uses the fact that at high energies, the transferred momentum for pp elastic scattering is nearly transverse. This establishes the optimal condition for suppressing the SRC effect as $\vec{p}_{ft} \sim -\vec{p}_{rt}$.

- To ensure registration of events dominated by screening and double scattering effects we restrict $200 \leq |\vec{p}_r| \leq 350 - 400$ MeV/c.

In conclusion, the following are the principal kinematical requirements for performing the proposed measurements:

$$\begin{aligned} \alpha \approx x \equiv \frac{Q2}{2m\nu} &\approx 1 \\ \nu - T_f - T_r - \frac{p_{A-2}^2}{2M_{A-2}} &\leq m_\pi \\ \vec{p}_{ft} &\approx -\vec{p}_{rt} \\ |\vec{p}_f| &\gg |\vec{p}_r| \\ 200 \leq |\vec{p}_{rt}| &\leq 400 \text{ MeV/c} \end{aligned} \tag{13}$$

The above kinematics define the two angular cones for knocked-out and secondary protons with respect to the direction of the virtual photon; this is demonstrated in Fig. 13.

3.2. Acceptance and Resolution

The high-efficiency of CLAS for multiple particles in the final state makes it ideally suited for these studies and essential for the case of ^{3}He. We have studied $^3\text{He}(e, e'pp)$ in detail using constraints on the regions of maximum theoretical interest: $0.9 < x < 1.1$, $0.2 < p_r < 0.6$ GeV/c recoil proton momentum, $40° < \theta_r < 130°$ recoil proton angle, and $15° < \theta_f < 40°$ struck proton angle, all measured in the laboratory frame. Events from our Monte Carlo generator were run through SDA and then reconstructed. Fig. 14 shows a typical reconstructed event in which an electron (1) is detected in coincidence with a fast proton (2) and a recoil proton (3). The combined 3-particle efficiencies for $4.5 < Q^2 < 5.5$ are shown in Fig. 15 as a function of fast proton angle (upper curve) and recoil proton angle (lower curve). Over our range of interest, the acceptance is reasonably flat and quite large. Studies of the average acceptance as a function of Q^2 yield 0%, 12.5%, 48.3%, and 51.0% for $Q^2 = 1$, 2, 5, and 6 GeV^2, respectively.

Proposal 94-102[64] gives the overall acceptances for $\text{d}(e, e'p_{\text{back}})$ as a function of p_{back} at $Q^2 = 2$ GeV^2. The number is consistently about 50% over the range $0.2 < p_{\text{back}} < 0.6$

GeV/c and also improve with increasing Q^2. Detection of a fast forward-moving proton has a similar acceptance.

Since both acceptance and missing-mass resolution degrade with increasing number of particles in the final state, we will concentrate on the case of ^{3}He. Proposal 94-102[64] already lists comparable results for the deuteron. Because $^3\mathrm{He}(e,e'pp)$ is kinematically complete, the reconstruction of the mass, momentum and emission angle of the undetected neutron is possible. Fig. 16 shows the reconstructed neutron mass (upper plot) and the deviation of reconstructed neutron angle from its true value (lower plot). The corresponding widths of the distributions are $\sigma = 12$ MeV (mass) and $\sigma = 2.6°$ (angle). This is more than sufficient to insure quasielastic kinematics with no contamination from inelastic processes. Moreover, all double scattering effects vary slowly compared to the scale of the experimental angular resolution.

3.3. Counting Rate

Deuteron target

For the deuteron target we would like to measure the Q^2 dependence of the ratio defined according to Eq. 9 where σ^{double} is the measured cross section from the kinematical region dominated by double scattering and $\sigma^{screening}$ is from the kinematical region corresponding to a dominant contribution from the interference between PWIA and rescattering amplitudes. As it follows from Fig. 4 (see Ref.[41] for detailed discussions) the kinematics where $x \approx \alpha_r \approx 1$ and $p_{rt} = 200$ MeV/c defines the dominant contribution from screening effects, and $p_{rt} > 300$MeV/c the dominant contribution from double scattering effects. Thus we are considering the ratio of $\sigma(p_{rt} = 300, 400 \text{ MeV/c})/\sigma(p_{rt} = 200 \text{ MeV/c})$ at the following kinematical ranges:

$$Q^2 = Q_0^2 \pm 0.5 \text{ GeV}^2 \quad x \approx \alpha = 1 \pm 0.15 \quad |p_{rt}| = 0.2,\ 0.3,\ 0.4 \pm 0.05 \text{ GeV/c}. \qquad (14)$$

The kinematics of the knock-out nucleon is determined by energy-momentum conservation. Note that all angles are defined in a coordinate system where the z-axis is along $\vec{q}$. The calculation of $d(e,e'p)n$ cross section, where proton registered at forward kinematics, according to the code developed in Ref.[41], averaged within these kinematical ranges gives following estimates at $Q_0^2 = 5$ GeV^2:

$$\begin{aligned}
\frac{d\sigma}{dQ^2 dx d\phi_e dp_{rt} d\phi_r} &= 0.1725 \times 10^{-3} \frac{nb}{GeV^3 rad^2}(p_{rt} = 200 MeV/c) \quad (Eikonal\ \ approx.) \\
&= 0.4548 \times 10^{-4} \frac{nb}{GeV^3 rad^2}(p_{rt} = 300 MeV/c) \quad (Eikonal\ \ approx.) \\
&= 0.2385 \times 10^{-4} \frac{nb}{GeV^3 rad^2}(p_{rt} = 400 MeV/c) \quad (Eikonal\ \ approx.) \\
&= 0.1865 \times 10^{-3} \frac{nb}{GeV^3 rad^2}(p_{rt} = 200 MeV/c) \quad (QDM - CT\ model) \\
&= 0.4187 \times 10^{-4} \frac{nb}{GeV^3 rad^2}(p_{rt} = 300 MeV/c) \quad (QDM - CT\ model)
\end{aligned}$$

$$= \quad 0.2045 \times 10^{-4} \frac{nb}{GeV^3 rad^2} (p_{rt} = 400 MeV/c) \quad (QDM - CT\ model) \tag{15}$$

where the estimation of the cross section with CT effects is done within the quantum diffusion model (see Eqs. 5–6). Using the kinematical intervals of Eq. 14, the beam luminosity L $= 10^{34}/\mathrm{cm}^2/\mathrm{s}$ [65] and the acceptance $\sim 70\%$ one obtains the following counting rate at $p_{rt} = 400\ MeV/c$:

$$\begin{aligned} N_{rate} &\approx 0.68 \text{ events per hour} \quad (Eikonal\ \ approximation) \\ &\approx 0.58 \text{ events per hour} \quad (QDM - CT\ model) \end{aligned} \tag{16}$$

Under these conditions, ~ 400 hours of beam-time is required on the deuteron to acquire $\sim 270(230)$ events at $Q^2 = 5$ (GeV/c)^2 ($\pm 6\%$ statistical error). Fig. 17 shows the predicted ratio of cross sections under these kinematical constraints.

^{3}He and ^{4}He targets:

The starting point for estimating the counting rates is the requirement for obtaining better than 10% statistical accuracy at $Q^2 = 5$ GeV^2 for the measurements of the ratio of $(e, e'pp)$ events defined by the kinematics of Eq. 13 (see Fig. 13), to the (e, ep) events obtained in the small angular cone (see Fig. 13) (without any constraints on the transverse momenta of knocked-out protons). This measurement is proposed for the ^{3}He target at the electron beam energy $E_e = 6$ GeV. The average acceptance for three prong events is about 50%. This value of the acceptance is consistent with the requirements for the proposed experiment.

Since the cross section for $(e, e'pp)$ is small with respect to the $(e, e'p)$ reaction the overall accuracy will be determined by the accuracy of the double scattering measurement.

For estimating the cross section for the $(e, e'pp)$ reaction we have used the results from the following different approaches: three-state model and the quantum diffusion model of CT[43], and the conventional Glauber approximations[34]. All models agree with the experimental data for semiexclusive $(e, e'p)$ processes[22,62,63] after summing over all quasielastic states of the residual hadronic system.

To estimate the expected counting rate of $(e, e'pp)$ events, we estimate the cross section integrated over the following kinematical ranges

$$\begin{aligned} Q^2 = Q_0^2 \pm 0.5 \mathrm{GeV}^2 \qquad & x = 1 \pm 0.1 \qquad & \alpha_r = 1 \pm 0.1 \\ |p_{rt}| = 0.4 \pm 0.05 \text{ GeV/c} \quad & |p_{ft}| = 0.4 \pm 0.05 \text{ GeV/c} \quad & |\phi_r - \phi_f| = 180 \pm 30^0. \end{aligned} \tag{17}$$

This gives the following value of the averaged cross section at $Q_0^2 = 5$ GeV^2:

$$\begin{aligned} \frac{d\sigma}{dQ^2 dx d\phi_e d\alpha_r dp_{rt} d\phi_r dp_{ft} d\phi_f} &= 2.59 \times 10^{-3} \frac{nb}{GeV^4 rad^2} \quad (Eikonal\ \ approx.) \\ &= 1.98 \times 10^{-3} \frac{nb}{GeV^4 rad^2} \quad (QDM - CT\ model), \end{aligned} \tag{18}$$

where the cross section with CT effects is estimated using the quantum diffusion model (see Eqs. 5–6). Using the kinematical intervals of Eq. 17, the beam luminosity L $= 10^{34}/\mathrm{cm}^2/\mathrm{s}$ [65] and the acceptance $\sim 50\%$ one obtains the following counting rate for $N_{e,e'pp}$ events:

$$\begin{aligned} N_{e,e'pp} &\approx 0.77 \text{ events per hour} \quad (Eikonal\ \ approximation) \\ &\approx 0.59 \text{ events per hour} \quad (QDM - CT\ model) \end{aligned} \tag{19}$$

Under these conditions, ~ 200 hours of beam-time is required on ^{3}He to acquire $\sim 160(120)$ events at $Q^2 = 5$ (GeV/c)^2 ($\pm 8(9)\%$ statistical error). We have estimated, that the rate of the (e,e'pp) reaction on the ^{4}He is about the same as for ^{3}He, because the factor of a smaller radius of ^{4}He will be compensated by extra screening due to the extra neutron.

In Fig. 18 the expected effects of color transparency are presented with statistical errors only.

3.4. Backgrounds

The physical background of double scattering events is due to various mechanisms such as meson exchange currents, isobar contributions and off-shell effects considered in section 2.4. We set $10 - 15\%$ as the upper limit of these uncertainties. This is because there are smaller MEC, IA and off shell effects at the relatively large values of Q^2 we encounter here. Moreover the relatively high rates (see above) and negligible CT effects at $Q^2 = 1 - 2$ GeV^2 provides important information about these effects, which we can use to interpret the data at higher Q^2.

Combinatorial backgrounds in this experiment will be similar to Experiment 94-102[64] on the deuteron. In that case, secondary interactions of knocked-out protons in the target material and walls were found to be negligible. Accidental coincidences between electrons and uncorrelated proton tracks are the dominant source of background. In the deuteron case, we have estimated the number of events for $Q^2 > 1$ with a good electron but no proton; $Q^2 < 1$ with no electron but a proton somewhere; and $Q^2 < 1$ with no electron and only a backward-going proton. The corresponding counting rates 590, 63000 and 2400 per second, a resolving time of 1–2 ns, and a true event rate of about 2 per second can be combined using the relation accidental/true $= R_{\mathrm{nop}} R_{\mathrm{noe}} \Delta T / R_{\mathrm{true}}$. This yields accidental/true ratios of about 10^{-3} for events with backward-going protons and a factor of 20 larger for events with a proton anywhere. Backgrounds such as these on the level of a few percent will not influence the results, especially since tight missing mass cuts for quasi-elastic kinematics will reduce this number considerably. Estimates using CELEG for ^{3}He are similar.

3.5. Beam Time Request

For the measurements on D at 6 GeV, the authors will cooperate with proposal[64] 94-102. The 400 hours already allocated is ample for this purpose. New time of 200 hours for ^{3}He at 6 GeV is requested. Running on ^{4}He will be used to check the reliability of the Glauber calculations before CT sets in using 60 hours of already approved time at 4 GeV.

Target	Total (hours)	Approved (hours)	Requested (hours)
D at 6 GeV	400	400	–
^{3}He at 6 GeV	200	–	200
^{4}He at 4 GeV	60	60	–

4. Summary

The Q^2 - dependence of the ratio of the yields in $(e, e'NN)$ and $(e, e'N)$ reactions on D, ^{3}He and ^{4}He targets is proposed to be investigated with the CLAS detector using the 6 GeV electron beam of CEBAF. Scattered electrons will be detected in the range of $Q^2 = 1 - 6$ $(\mathrm{GeV/c})^2$ in coincidence with one or two protons in quasielastic kinematics. These data will allow the dynamics of color coherence phenomena to be studied. The effect should be observed at $Q^2 \sim 3 - 6$ $(\mathrm{GeV/c})^2$.

These proposed studies will improve our understanding of nonpertubative QCD dynamics. The systematic investigation of processes at Q^2 starting from 1 $(\mathrm{GeV/c})^2$ below the onset of color transparency will provide solid data on the relevant nuclear effects as well. Comparing the results for D and ^{3}He will considerably improve the reliability of the analysis.

5. References

1. K. Rajagopal and F. Wilczek, *Nucl.Phys.* **B399**, 395 (1993).
2. A. Mueller, in *Proceedings of the 17 Rencontre de Moriond* edited by J. Tranh Thanh Van (Editions Frontieres, Gif-sur-Yvette, 1982), p.13.
3. S.J. Brodsky, in *Proceedings of the Thirteenth International Symposium on Multiparticle Dynamics*, edited by E.W. Kittel, W. Metzger, and A. Stergiou (World Scientific, Singapore, 1982), p.964.
4. H.N. Li and G. Sterman *Nucl.Phys.* **B381**, 129 (1992).
5. L.L. Frankfurt and M.I. Strikman, in *Progress in Particle and Nuclear Physics*, v.**27**, p.135(1991).
6. L.L. Frankfurt and V. Khoze, Proceedings of X LNPI Winter school, v.2, 196-408,1975
7. M. Derrick et al., DESY 95-133, 1995.
8. S. J. Brodsky , L. L. Frankfurt, J. F. Gunion, A. H. Mueller and M. I. Strikman Phys.ReV. **D50**, 3134 (1994).
9. L. L. Frankfurt, W. Koepf and M. I. Strikman, Hep-ph 9509311, 1995.
10. L.L. Frankfurt and M.I. Strikman, Nucl. Phys., **B250**, p.143(1985)
11. L.L. Frankfurt and M.I. Strikman, *Phys. Rep.*, **76**, 215(1981)
12. L.L. Frankfurt and M.I. Strikman, *Phys. Rep.*, **160**, 237(1988)
13. G.R. Farrar, L.L. Frankfurt, M.I. Strikman and H. Liu, Phys. Rev. Lett., **61**, 686(1988).
14. B.K. Jennings and G.A. Miller, Phys. Lett., **B236**, 209(1990); B.K. Jennings and G.A. Miller, Phys. Rev., **D 44**, 692(1991); Phys. Rev. Lett., **70**, 3619(1992); Phys. Lett., **B274**, 442(1992); Phys. Lett., **B318**, 7(1993).
15. L.L. Frankfurt, G.A. Miller, and M.I. Strikman, *Comments on Particle and Nuclear Physics*, v.**21**, p.1(1992); L.Frankfurt, G. A. Miller, and M.Strikman, Nucl. Phys. A555(1993)752-764.
16. L.L. Frankfurt, M.I. Strikman and M. Zhalov, Nucl. Phys., **A515**,599(1990).
17. J.P. Ralston and B. Pire, Phys. Rev. Lett., **61**, 1823(1988). B. Pire and J.P. Ralston, Phys. Lett.,**117B**, 233(1982)
18. O. Benhar *et al.* Phys. Rev. Lett., v.**69**, 881(1992).
19. T.-S.H. ,Lee and G.A. Miller, Phys. Rev. C45,1863(1992).
20. L.L. Frankfurt, M.I. Strikman and M. Zhalov, *PSU preprint* 1993, Phys.Rev.C to be published.
21. A.S. Carroll *et al.* Phys. Rev. Lett., **61**, 1698(1988).
22. N.C.R. Makins et al. Phys. Rev. Lett. **72**, 1986 (1994).
23. A.S. Carroll *et al.*, BNL experiment 850.
24. M. R. Adams, et al. Phys.Rev.Lett., **74**, 1525 (1995).
25. N.Isgur, Summary talk at Baryons 95.
26. B.L.Ioffe and A.V.Smilga, *Phys. Lett.* **B114**, 353(1982).
27. V.A. Nesterenko and A.V. Radyushkin, *Phys. Lett.*, **B115**, 410(1982):

A.V. Radyushkin, *Acta Phys. Polon.* **B15**, 403(1984);
G.P. Korchemski and A.V. Radyushkin, *Sov. J. Nucl. Phys.*, **45**, 910(1987).
28. N. Isgur and C.H. Llewellyn-Smith, *Phys. Rev. Lett.* **52**, 1080(1984); *Phys. Lett.* **B217**, 535(1989).
29. L.L. Frankfurt, G.A. Miller, and M. Strikman, *The Geometrical Color Optics of Coherent High Energy Processes* Ann. ReV. of Nucl. and Particle Phys. **44**, 501 (1994).
30. E.J.Moniz, G.D.Nixon, *Phys. Lett.* **30B**, 393 (1969); E.J.Moniz, G.D.Nixon and J.D.Walecka, *Effect of Correlations on High-Energy Processes Using Nuclear targets* 1970.
31. D.R.Yennie in *Hadronic Interactions of Electrons and Photons* ed. J.Cummings, D.Osborn, 321(1971).
32. N.N. Nikolaev, A. Szczurek, et al. *Phys. Lett.* **B317** 287(1993).
33. A. Kohama, K. Yazaki and R. Seki, *Nucl.Phys.* **A551** 687 (1993).
34. L.L. Frankfurt, E. J. Moniz M.I. Strikman and M.M. Sargsyan Phys. Rev. **C51**, 3436 (1995).
35. L.L. Frankfurt, W.R. Greenberg, G.A. Miller, and M.I. Strikman, Phys. Rev., **C46**, 2547(1992).
36. M. Lacombe, B. Loiseau, R. Vinh Mau, J. Cote, P. Pires, R. de Tourreil; Phys. Let. **B101**, 139 (1981).
37. R. Machleidt, K. Holinde, C. Elster; Phys. Rep. **149**, 1 (1987).
38. J. Friar B.F. Gibson and G.L. Payne Phys. Rev **C24**, 2279 (1981).
39. W. Glökle and H. Kamada, Nucl. Phys. **A560**, 541 (1993).
40. J. Carlson and R. Schiavilla, in Few Body Systems Suppl. **7**, 1994, p.349; B.S. Pudliner, V. R. Pandharipande, J. Carlson and R. B. Wiringa, Nucl-Th - 1995.
41. L.L. Frankfurt, W.R. Greenberg, G.A. Miller, M. M. Sargsyan and M.I. Strikman, Z. Phys., **C46**, 2547(1995).
42. M. L. Frank, B. K. Jennings, G.A. Miller DOE/ER/40427-15-N95, DOE/ER/40561-217-INT95-00-99, nucl-th/9509030
43. K.Sh. Egiyan, L.L. Frankfurt, W.R. Greenberg, G.A. Miller, M.M. Sargsyan, and M.I. Strikman, CEBAF Preprint, PR-93-002; Nucl. Phys. **A580**, 365, (1994).
44. H. Arenhövel, in *Modern Topics in Electron Scattering*, Edited by B. Frois and I. Sick, 1991, p.136.
45. H. Arenhoevel, W. Leidemann, E. L. Tomusiak, *Phys. Rev.* **C46** 455 (1992).
46. P. Stoler *Phys.Rep.* **226** 103 (1993).
47. T.E.O. Ericson and W. Weise "Pions ans Nuclei" Oxford, UK: Clarendon (1988) 479p.
48. L.L. Frankfurt, W.R. Greenberg, G.A. Miller, M. M. Sargsyan and M.I. Strikman, DOE-Preprint, (1995), to be published in Phys. Lett. B.
49. C.Ciofi degli Atti, L. L. Frankfurt, S. Simula and M. I. Strikman, **C44**, R7 (1991).
50. L. L. Frankfurt, V. R. Pandharipande, M. M. Sargsyan, R. Schiavilla, M. I. Strikman, O. Benhar, *in progress.*

51. S.C. Pieper, *Private Communication.*
52. T. de Forest, *Nucl. Phys.* **A392** 232 (1983).
53. K. Sh. Egiyan and M. M. Sargsyan CEBAF preprint-9301 1993.
54. E. D. Bloom and F. Gilman *Phys. Rev.* **D4** 2901 (1971).
55. G. F. Bertsch L. L. Frankfurt and M. I. Strikman *Science* **259** 773 (1993).
56. G. E. Brown, M. Buballa, Zi Bang Li and J. Wambach SUNY-NTG-94-54, October 1994.
57. P. F. Shepard, T. J. Devlin, R. E. Mischke, J. Solomon, *Phys. Rev.* **D10** 2735 (1974).
58. I. P. Auer, *et al*, *Phys. Rev. Lett.* **46** 1177 (1981).
59. D. Joyce, *CELEG* CLAS-NOTE-006, CEBAF, (1989).
60. M.M. Sargsyan, *Electron Nucleon Generator* CLAS-NOTE-008, CEBAF, (1992).
61. CLAS event simulation code.
62. K.V. Alanakyan, M.J. Amaryan, G.A. Asryan *et al.*, Preprint YerPI, YERPHI-1303(89)-90.
63. M.M. Sargsyan, Preprint YerPI, YERPH-1331(26)-91
64. S.E. Kuhn and K.A. Griffioen (Spokespersons) *Electron Scattering from a High Momentum Nucleon in Deuterium* CEBAF Proposal E-94-102 1994.
65. CEBAF Conceptual Design Report, April 13, 1990 (Revised).

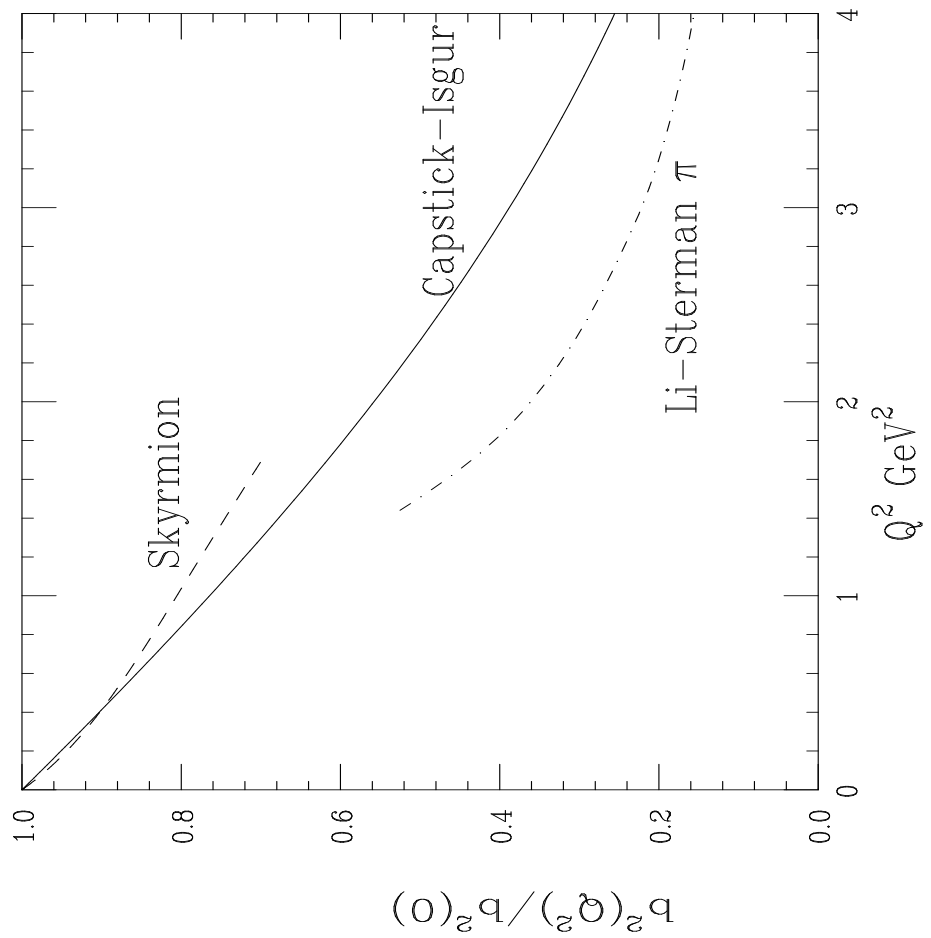

Fig. 1 Q^2-dependence of the hadronic transverse size for two models of the nucleon and one model of the pion.

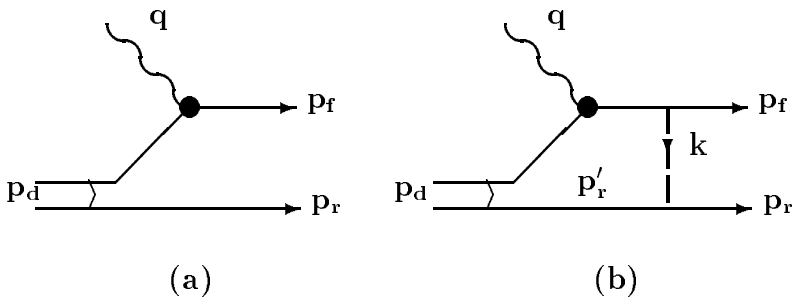

Fig. 2 Graphs for d(e,e'p)n scattering. (a) plane wave impulse approximation (PWIA); (b) final state interaction contribution, where the broken line accounts for all NN multiple scatterings.

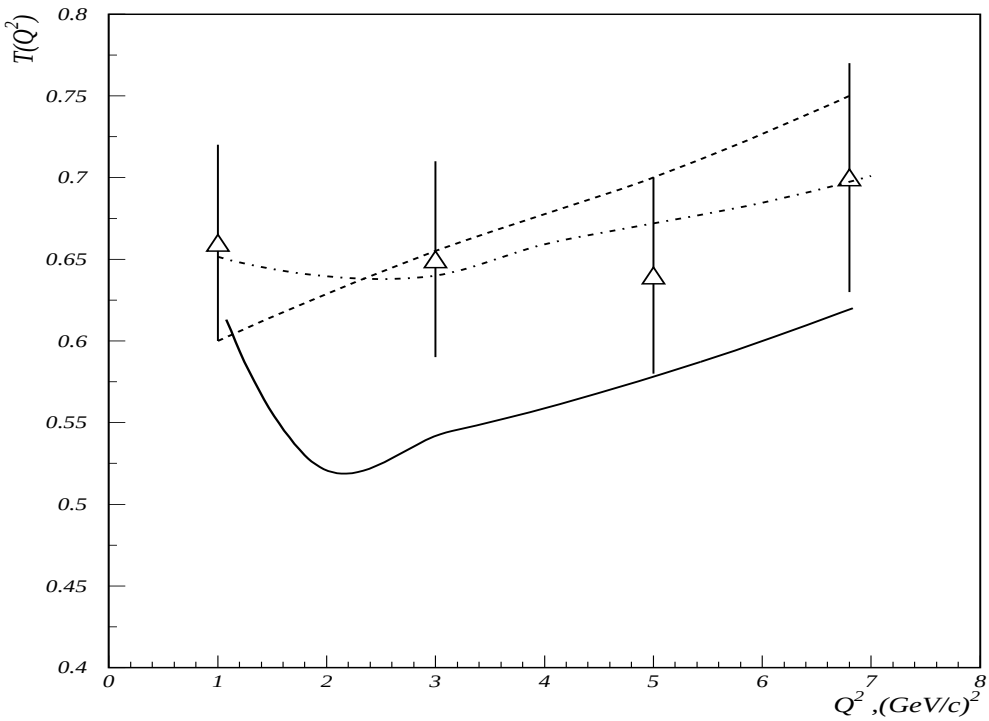

Fig. 3 NE18 data[22] together with predictions of the resonance model[14] (solid line), the color diffusion model including nucleon correlations[18] (dashed line), and the color diffusion model including correlations and nuclear-shell effects[34] (dash-dotted line).

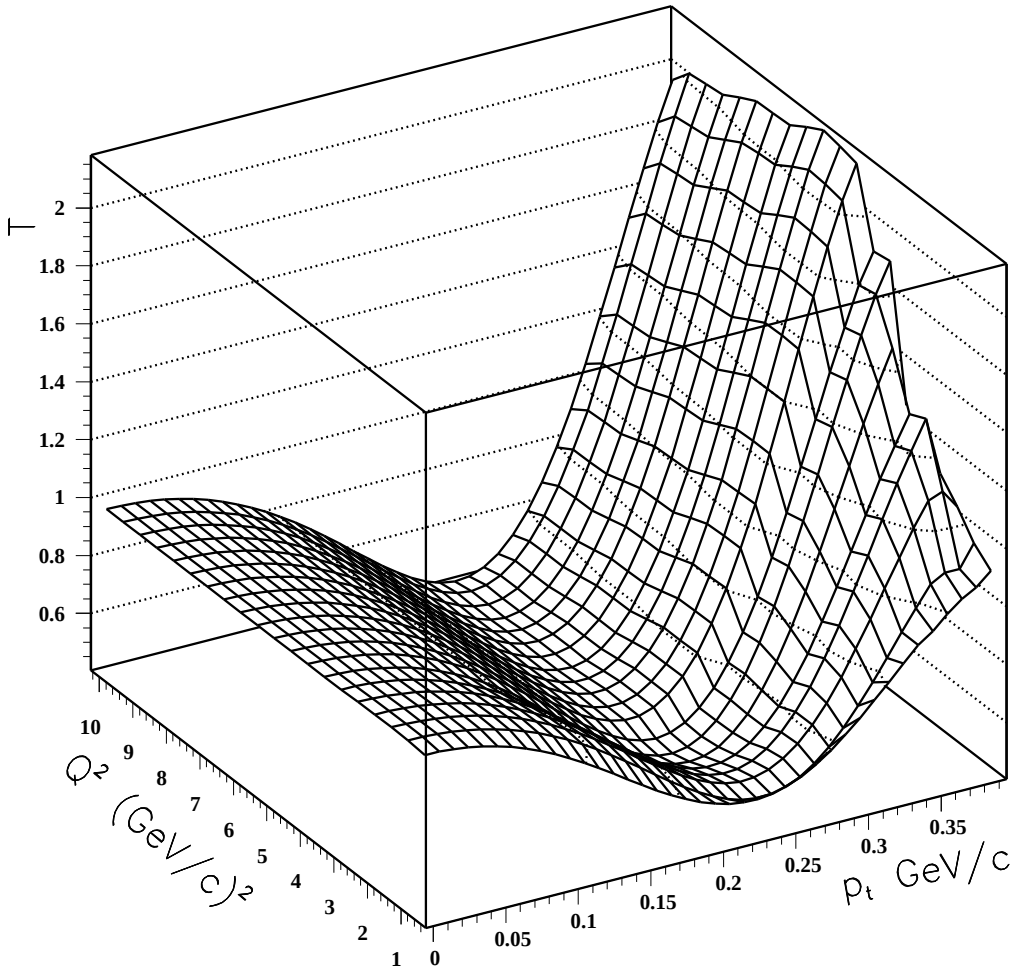

Fig. 4 T^{double} versus Q^2 and p_t at $\alpha = 1$ and $\vec{p}_r \approx p_t$.

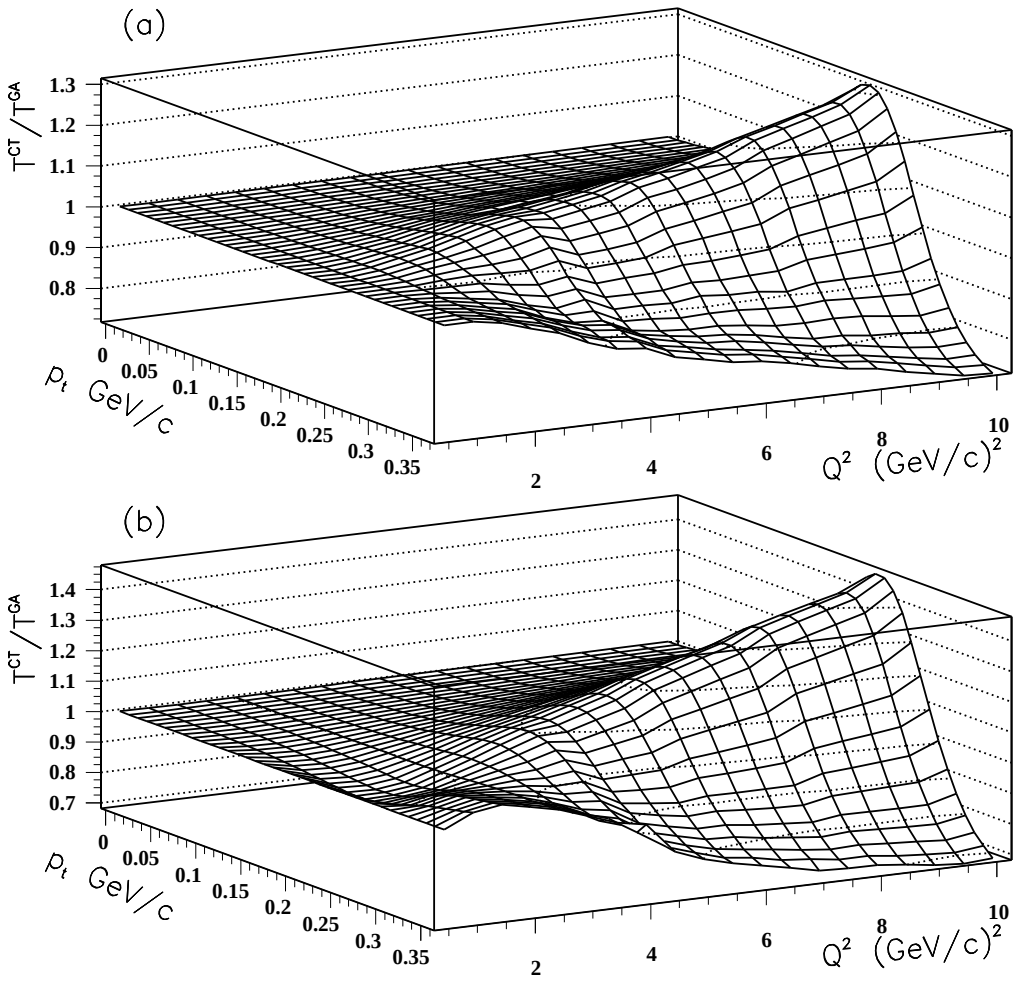

Fig. 5 The ratios $T_{CT}^{double}/T_{GA}^{double}$ versus p_t and Q^2 for $\alpha = 1$ as calculated in the (a) quantum diffusion and (b) three state models.

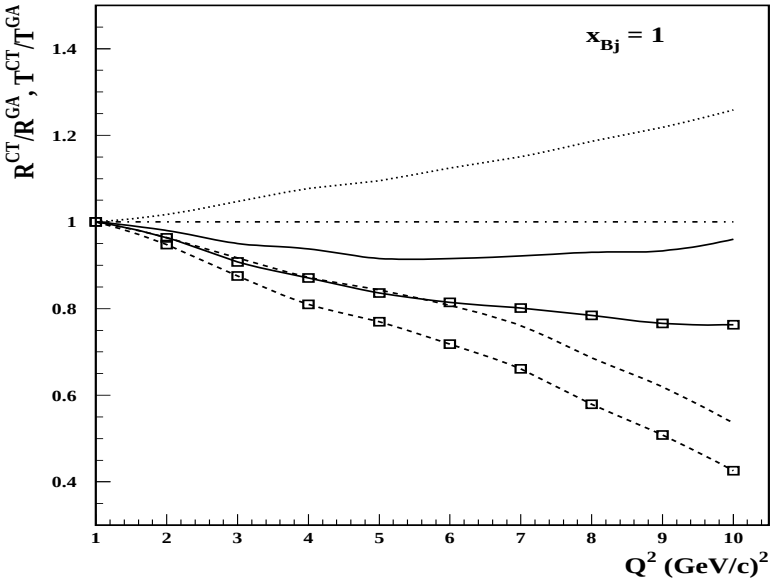

Fig. 6 The Q^2 dependence of the transparency T defined according to Eq. 7 and normalized to the GA calculations: dash-dotted line, GA approximation; dotted line, QDM prediction at p_r = 200 MeV/c; solid line, QDM prediction at p_r = 300 MeV/c; and dashed line, QDM prediction at p_r = 400 MeV/c. The curves labeled by boxes correspond to the Q^2-dependence of the QDM predictions for $R(Q^2, p_{r1}, p_{r2})$ defined according to Eq. 9 and normalized to the GA calculations. Solid line with "boxes", $p_{r1} = 300\ MeV/c$, $p_{r2} = 200\ MeV/c$; and dashed line with "boxes", $p_{r1} = 400\ MeV/c$, $p_{r2} = 200\ MeV/c$. QDM predictions were calculated with $\Delta M^2 = 0.7$ GeV^2 and $x = 1$.

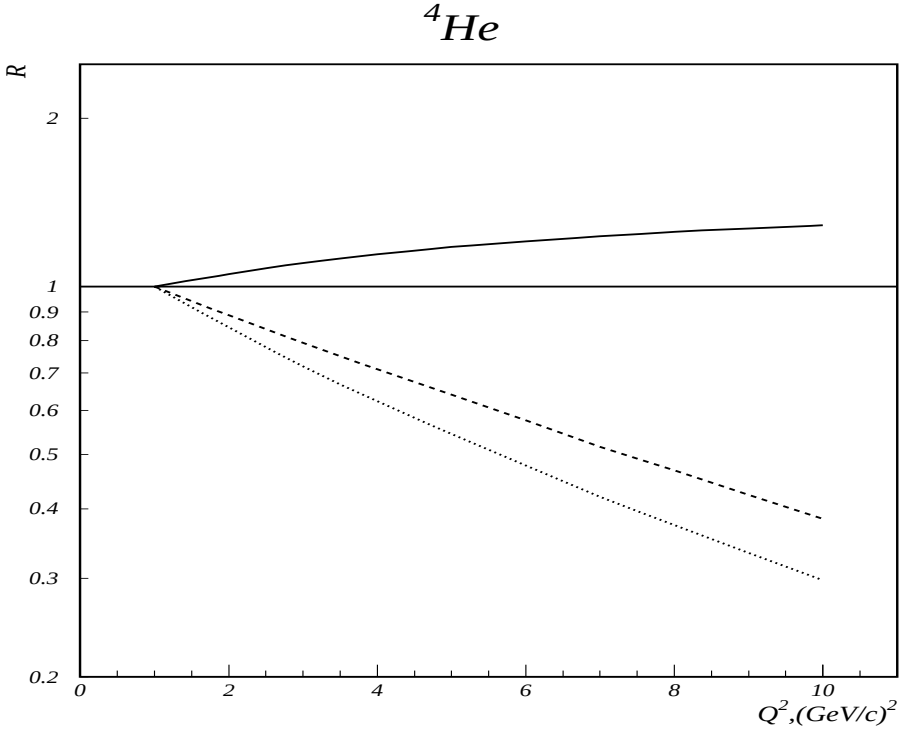

Fig. 7 The calculation of T (solid line), T^{double} (dashed line), R (dotted line) in the quantum diffusion model, normalized to the corresponding calculations in the Glauber approximation.

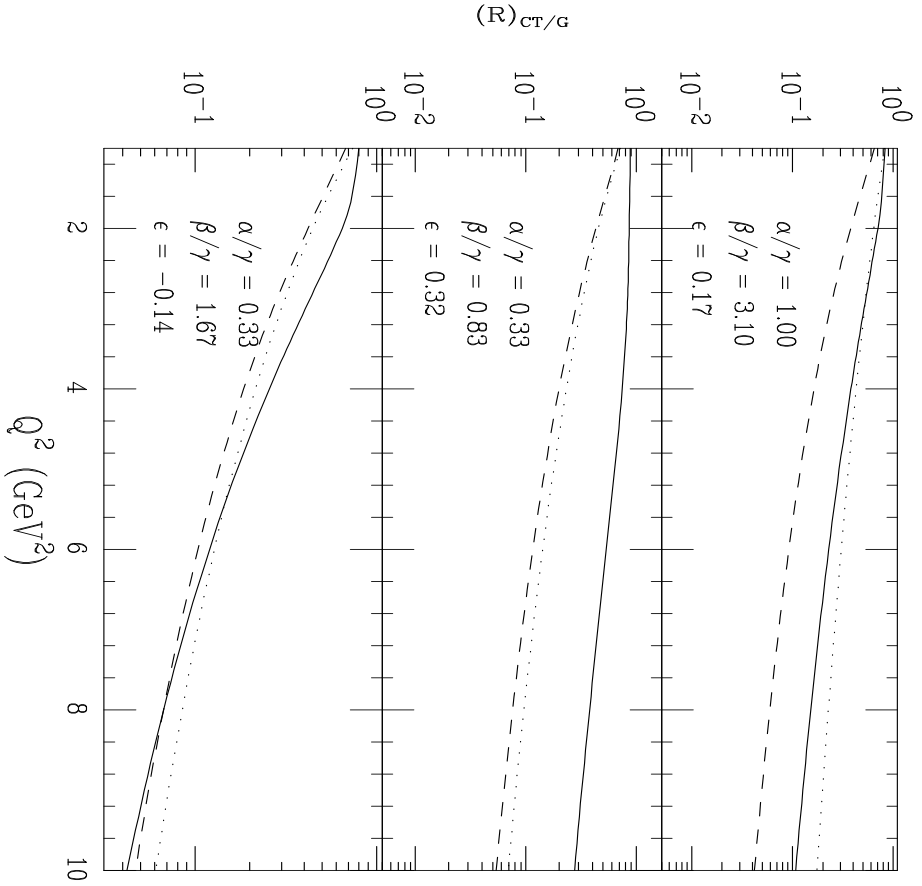

Fig. 8 R in the three-state model for ^{3}He. Dashed: quasielastic N^* (1.4 GeV) production. Dotted: quasielastic N^{**} (1.8 GeV) production. Solid: quasielastic N (0.938 GeV) production. The parameters α, β, γ and ϵ define the baryon-nucleon interaction[35].

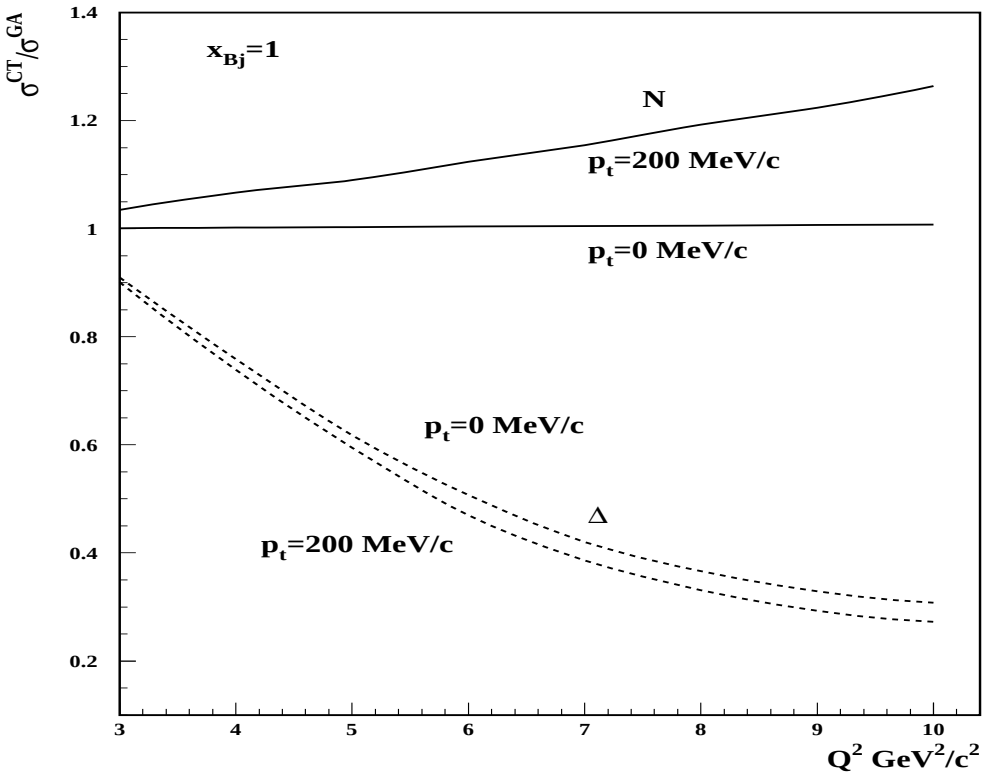

Fig. 9 The Q^2-dependence of the ratio of cross sections calculated within the QDM of color transparency to the cross section calculated within Glauber approximation. Pictured are the $d(e,e'N_1)N_2$ reaction (solid line) and the $d(e,e'N)\Delta$ reaction (dashed line).

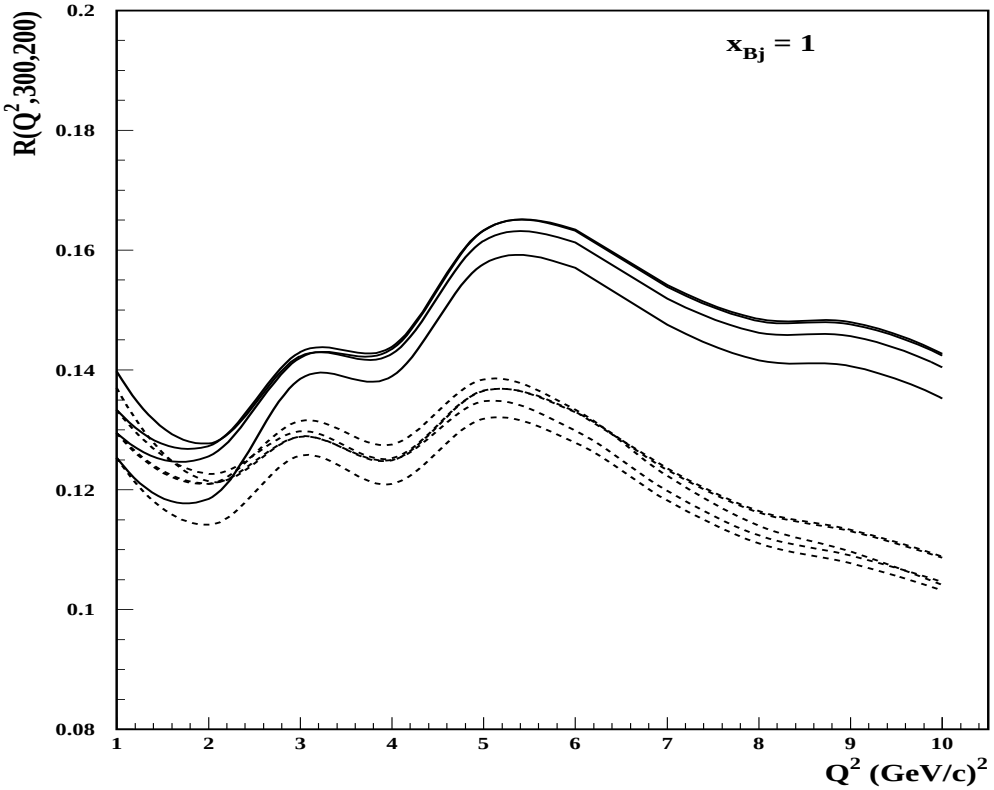

Fig. 10 The theoretical uncertainties in determining of Q^2-dependence of transparency $R(Q^2, p_{r1} = 300, p_{r2} = 200)$ at $x = 1$. The solid lines are Glauber approximations and the dashed lines are the QDM approximations. Upper and lower solid and dashed lines at $Q^2 = 1$ (GeV/c)^2 are the GA and QDM predictions with Paris and Bonn wave functions, respectively. The curves in between correspond to predictions with the Paris light cone wave function and predictions with a different approximation for electron- off-shell nucleon scattering σ_{en} (see e.g.[52,53]). Color screening effects appear at $Q^2 > 2$ (GeV/c)^2). The QDM is calculated with $\Delta M^2 = 0.7$ GeV^2.

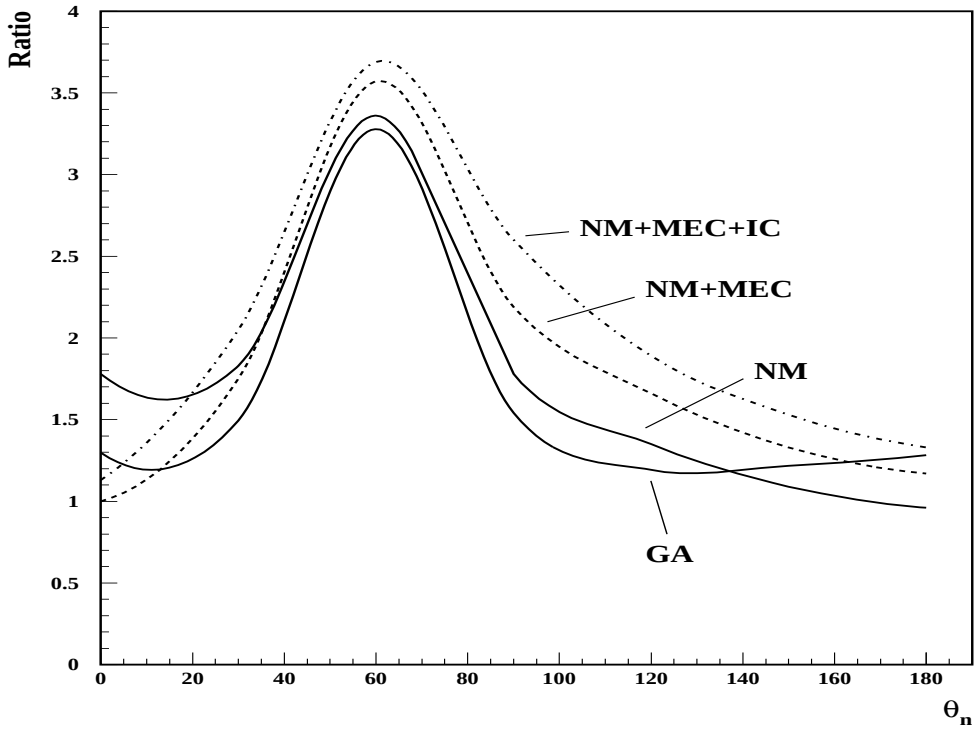

Fig. 11 The θ_n dependence of ratio R. Curve marked by GA shows the ratio of the $d(e,e'p)n$ cross section calculated within the eikonal approximation as derived in Ref.[41] and normalized to the PWIA cross section, NM is the cross section with multiple scattering and the Siegert operator normalized to the PWIA, which also accounts for the direct productions of slow neutrons, NM+MEC is the NM calculation with meson exchange currents, and NM+MEC+IC is the NM calculation with meson exchange currents and the isobar contribution. The last three curves are those of the calculation of Ref.[45] for $p_r = 400$ MeV/c and $Q^2 = 1$ (GeV/c)^2.

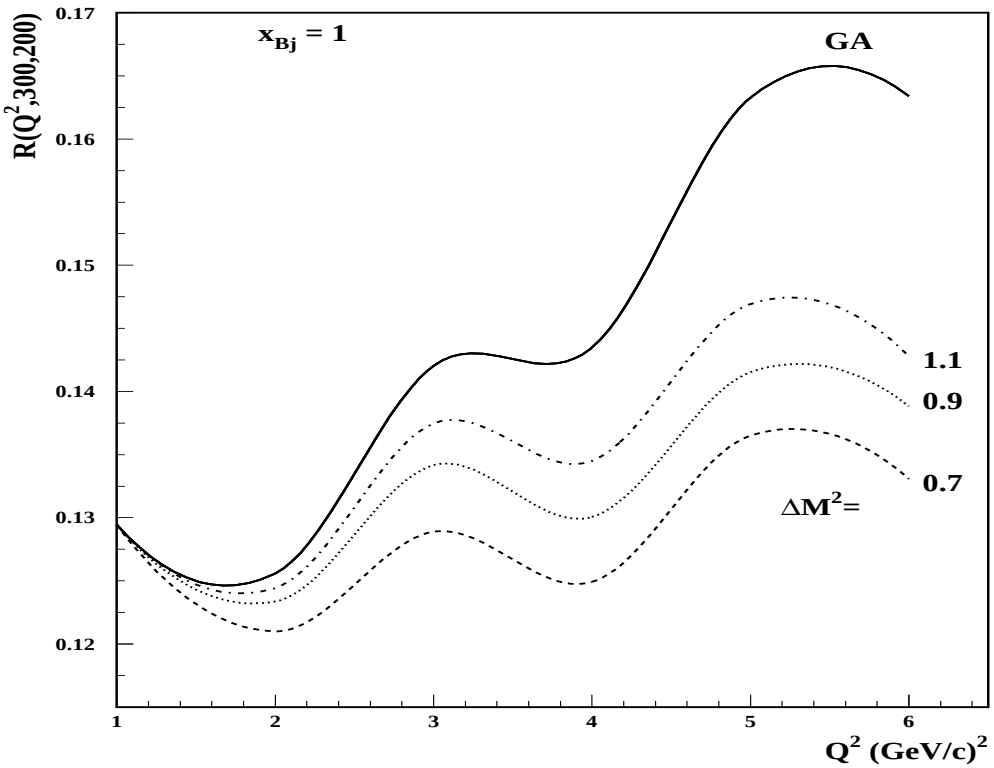

Fig. 12 The Q^2-dependence of the ratio $R(Q^2, p_{r1}, p_{r2})$ as defined according to Eq. 9 with $x = 1$, at $p_{r1} = 300$ MeV/c and $p_{r2} = 200$ MeV/c. The solid line is the Glauber approximation; the dashed line is the QDM approximation with $\Delta M^2 = 0.7$ GeV^2; the dotted line, $\Delta M^2 = 0.9$ GeV^2 and dash-dotted line, $\Delta M^2 = 1.1$ GeV^2.

..

Fig. 13 The geometry of the double-scattering ($ee'pp$) reaction.

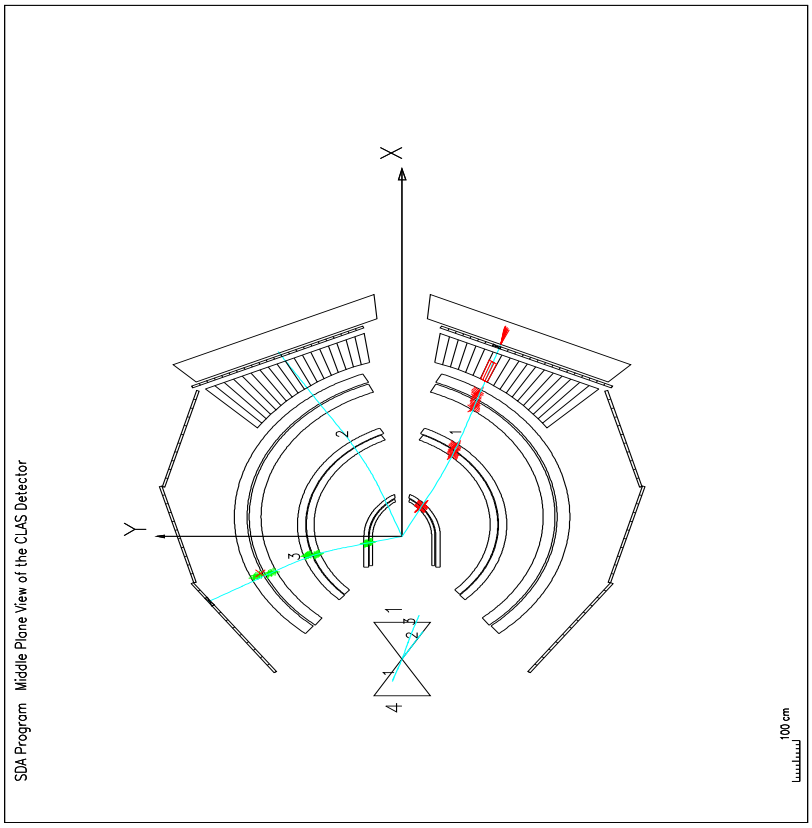

Fig. 14 A typical event as reconstructed in SDA. The electron (1) is observed in coincidence with a fast proton (2) and a slow recoil proton (3) for scattering on ^{3}He.

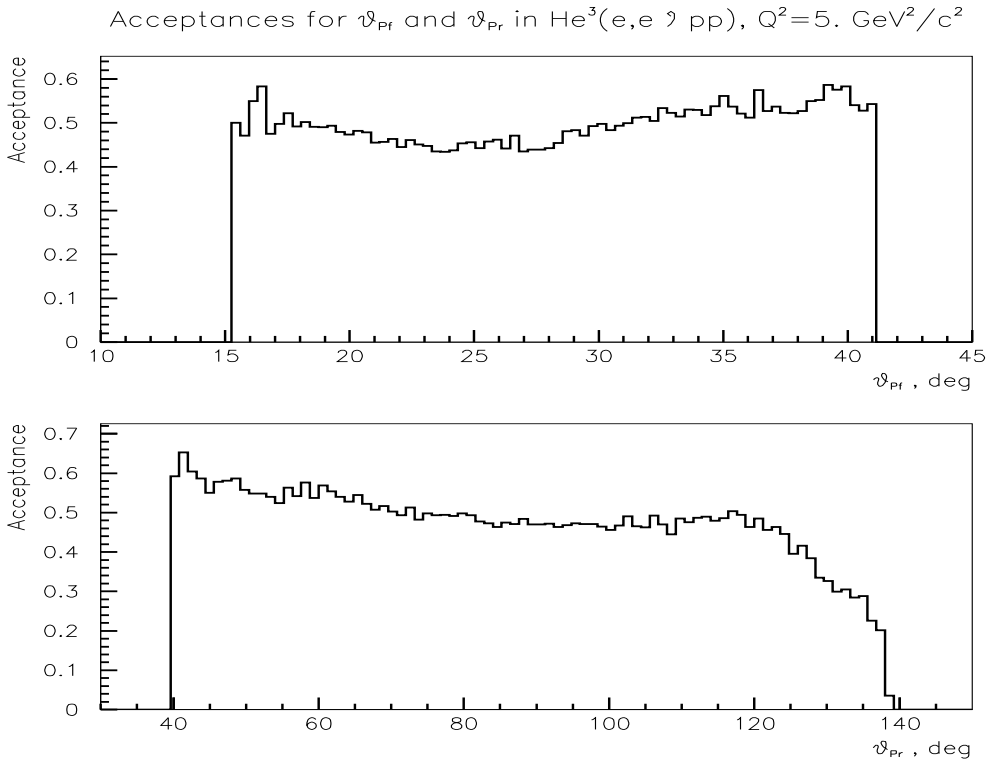

Fig. 15 Acceptances for ^{3}He$(e, e'p_f p_r)$ events as a function of the angle of the struck proton (upper plot) and of the recoil proton (lower plot) for $Q^2 = 5$ (GeV/c)^2. Over the region of interest, the acceptances are large and reasonably flat.

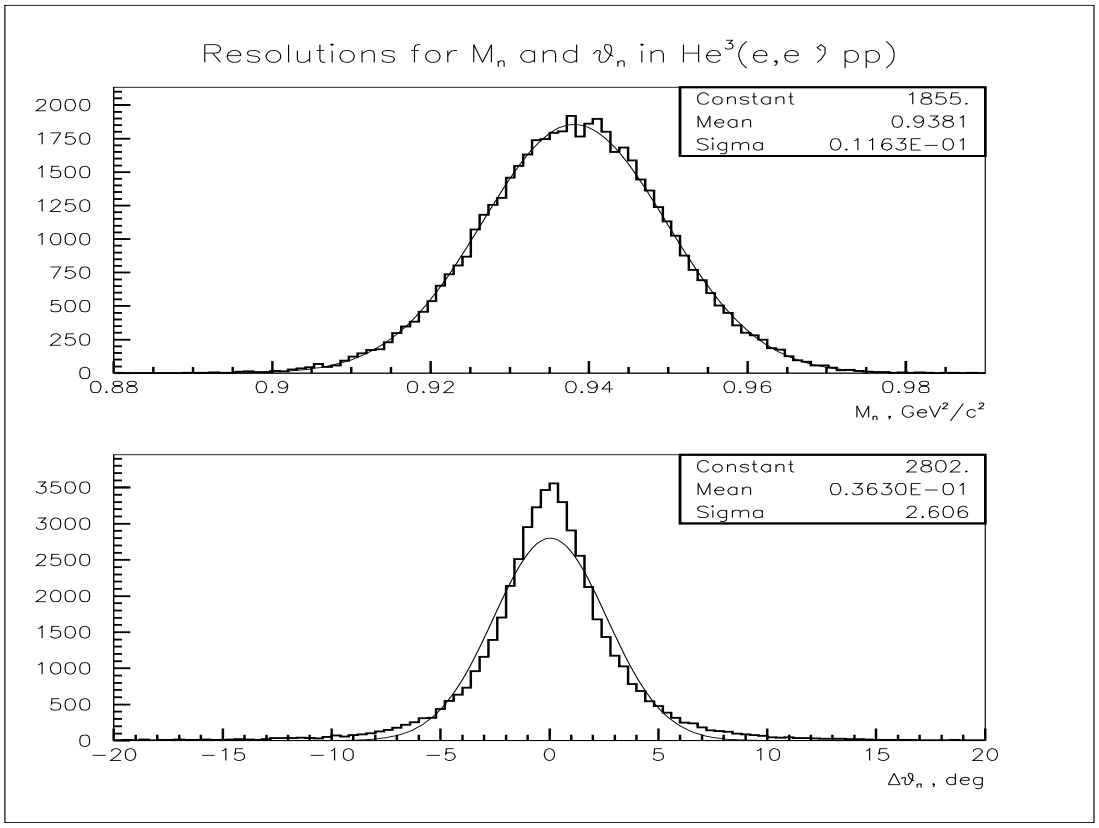

Fig. 16 Reconstructed mass resolution (upper plot) and angular resolution (lower plot) for the unobserved neutron in ^{3}He$(e,e'pp)$ reactions as determined with SDA.

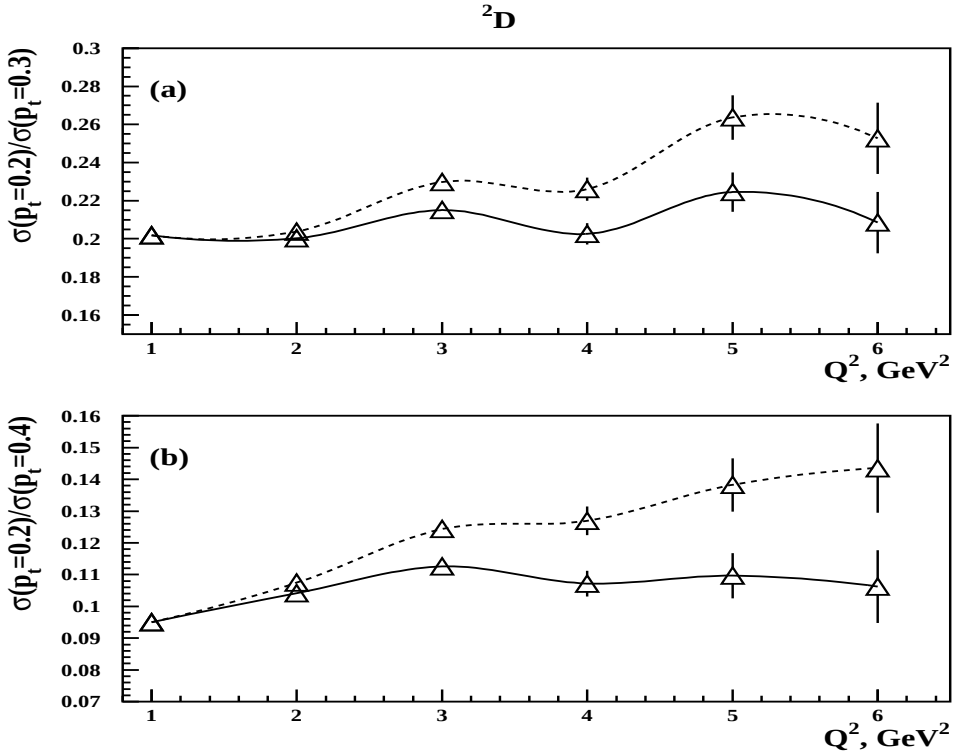

Fig. 17 Expected Q^2-dependence of the ratio $R(Q^2, p^t_{r1}, p^t_{r2})$ defined according to Eq. 9, at $p^t_{r1} = 300$ MeV/c and 400 MeV/c and $p^t_{r2} = 200$ MeV/c, with $x \approx \alpha_r = 1$. Solid line - CT prediction, dashed line - prediction of the Glauber approximation. Error bars correspond to statistical accuracy achieved with 400 beam hours at $10^{34}/\mathrm{cm}^2/\mathrm{s}$ luminosity.

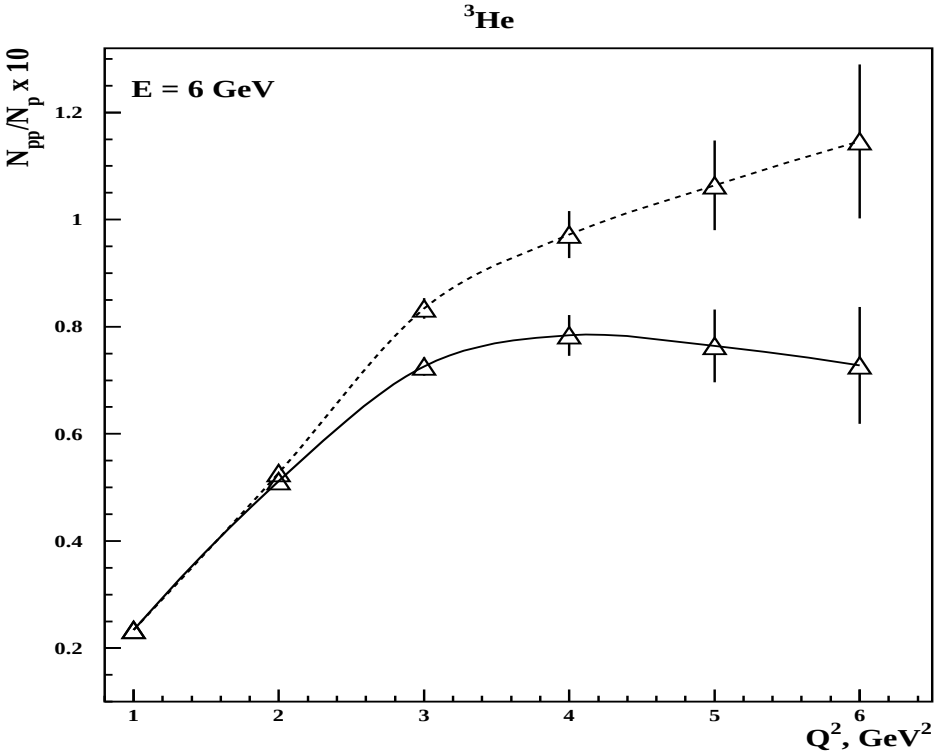

Fig. 18 Expected Q^2-dependence the ratio of $(e, e'pp)$ events to $(e, e'p)$ events. The kinematics are defined according Eq. 17. Solid line - CT prediction, dashed line - prediction of Glauber approximation. Error bars correspond to statistical accuracy achieved with 200 beam hours at $10^{34}/\mathrm{cm}^2/\mathrm{s}$ luminosity.